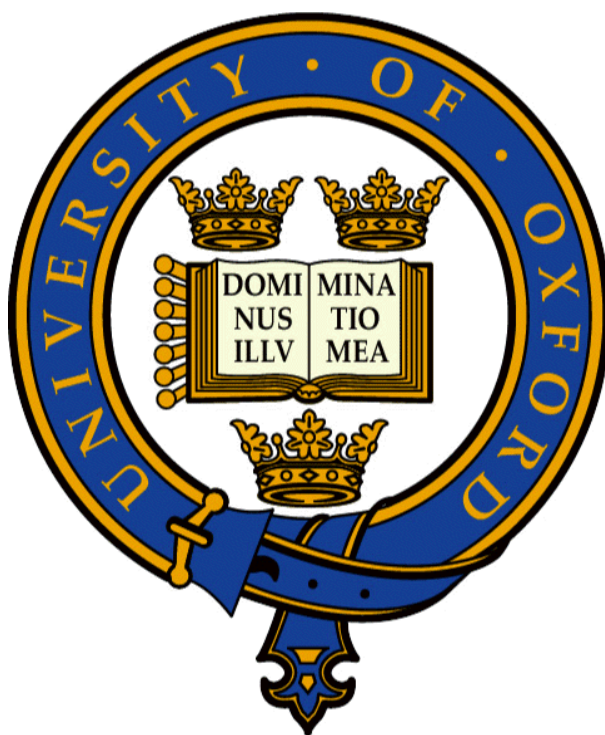


Morphology and Efficiency of Polymer:Fullerene Solar Cells

Richard Beal
Wolfson College



A thesis submitted for the Degree of
D.Phil. in Materials
University of Oxford

Abstract

This thesis seeks to describe the effects of thermal annealing on the morphology of polymer:fullerene solar cells and to develop P3HT:fullerene solar cells with improved efficiency. The first concern is addressed through the use of high resolution, low voltage, transmission electron microscopy (HRLVTEM) to directly image the morphology of P3HT:PCBM solar cells, on the nanometer scale, before, after and during the annealing process. The second focus is addressed through the use of modified anode layers, and more effectively, through the incorporation of novel fullerene derivatives into photovoltaic devices.

High resolution transmission electron micrographs of actual P3TH:PCBM devices are presented, providing direct evidence for the formation of P3HT and PCBM crystallites due to the annealing process. *In-situ* annealing of samples allowed unprecedented observation of the annealing process, revealing the mechanism of PCBM domain agglomeration in the P3HT:PCBM system. Experiments were also conducted to investigate vertical segregation within the films.

The improvement of polymeric anodes is of significant importance for the development of large area, efficient and flexible solar panels, and to that end, glycerol modified PEDOT was incorporated into P3HT:PCBM solar cells for the first time. The strategy proved ultimately unsuccessful, however the experiments did reveal some interesting

device physics which redefine the assumptions regarding the determination of the active device area.

The introduction of novel fullerene derivatives have the potential to significantly enhance the open circuit voltage of polymer:fullerene solar cells if the lowest unoccupied molecular orbital of the fullerene derivative is higher than that of PCBM. To this end a range of fullerene derivatives were subjected to cyclic voltammetry experiments to determine their LUMO levels relative to PCBM. Two candidates, bis-ThCBM and $\text{Er}_3\text{N@C}_{80}$ showed potential, with bis-ThCBM proving to be effective in bilayer photovoltaic devices. Bis-ThCBM was incorporated into optimized bulk heterojunction solar cells, achieving an efficiency of 4.6%, and a V_{OC} of 0.78V, one of the highest reported for a P3HT:fullerene solar cell. By way of comparison, P3HT:PCBM reference devices reached an efficiency of 3.6%.

The HRLVTEM techniques developed for this work have great potential for the investigation of novel polymer:fullerene morphologies and their responses to thermal annealing and ageing. In addition, the techniques are extendable to a wide range of organic thin films in which nanoscale morphology plays an important role. The identification of bis-ThCBM as an advanced electron acceptor has the potential to significantly advance state of the art solar cell efficiencies through its incorporation in devices with the next generation of semi-conducting polymers.

Acknowledgements

There are a significant number of people whose contributions to this thesis, large and small, deserve thanks:

Firstly, I thank the Rhodes Trust for allowing me to study at Oxford in the first place and for their financial and social support. I thank my supervisor Dr. Hazel Assender for giving me the freedom to enjoy so much of Oxford and for her many insights along the way. To my supervisor Dr. Andrew Watt, thank you for all his help and the TEM images. It has been quite a journey for both of us. Thank you to my collaborators Dr. Jamie Warner and Dr. Chris Blanford whose expertise in TEM modelling and cyclic voltammetry are greatly appreciated. Also, thank you to Dr. Kyriakos Porfyrakis who provided me with novel fullerenes fullerene derivatives and let me work in his labs. For this I must also thank Professor Andrew Briggs.

I must thank the post doctoral researchers and graduate students who I have worked with, especially Drs. Aaron Barkhouse and Helen Smith who showed me the ropes when I first arrived in the lab, and also Drs. Kiril Kirov, Alexandros Stavrinnadis and Jonathan Moghul. To Laura Droessler, Peter Kovacic, Shawn Willis and Elva Zou, thank you for making my last few months in the lab more enjoyable than they otherwise would have been.

Thank you to the Materials Department, and the people there without whom the whole place would grind to a halt; Lyn Richmond, Barry Fellows, Ian Sutton, Richard Cripps, Laurie Walton, Paul Warren and especially Richard Turner.

Penultimately, I thank my parents, who have provided so much great support during my DPhil, great patience as the thesis slowly wound to a close and great faith in booking their airfares for my graduation.

And of course, I thank my gorgeous and truly supportive girlfriend, Catherine, the best discovery I made at Oxford.

Declaration of Originality

This thesis is an account of work carried out by the author in the Materials Department, University of Oxford under the supervision of Dr. Hazel Assender and Dr. Andrew Watt. Where the work of others has been drawn upon this is duly acknowledged in the text, and a list of references is presented at the end of each chapter. No part of this thesis has been submitted towards the completion of another degree at the University of Oxford or elsewhere. Parts of this thesis have been submitted to or published in the following scientific journals or conference presentations:

R.M. Beal, J Moghal, C. Blanford, H.E. Assender and A.A.R. Watt, *On the enhanced open circuit voltage and efficiency of P3HT:bis-ThCBM solar cells*, in preparation

R. M. Beal, H.E. Assender, A.A.R. Watt, *Glycerol modified PEDOT:PSS anodes in P3HT:PCBM solar cells*, in preparation.

R.M. Beal, A. Stavrinadis, J.H. Warner, J.M. Smith, H.E. Assender and A.A.R. Watt, *The molecular structure of polymer-fullerene composite solar cells and its influence on device performance*, Macromolecules, doi: 10.1021/ma902211u

Alexandros Stavrinadis , **Richard Beal**, Jason M. Smith, Hazel E. Assender and Andrew A. R. Watt, *Direct formation of PbS Nanorods in Conjugated Polymer*, Advanced Materials, 20, 3105, (2008).

R.M. Beal, A. Stavrinadis, J.H. Warner, J.M. Smith, H.E. Assender and A.A.R. Watt, *Revealing the Morphology of P3HT:PCBM Bulk Heterojunction Solar Cells with in situ TEM*, 5th Photovoltaic Science, Application and Technology conference (PVSAT-5), Oral presentation.

R.M. Beal, H.E. Assender and A.A.R. Watt, *HRTEM analysis of bulk heterojunction morphologies with novel solvation*. Oral Presentation, SPIE Photonic West Conference 2008.

Table of Contents

Abstract	i
Acknowledgements	iii
Declaration of Originality	v
Table of Contents	vii
List of Abbreviations, Acronyms and Symbols	xi
I. Introduction	1
I.I Motivation	1
I.II History of Photovoltaics	2
II. Theoretical Review	6
II.I Photophysics of Polymer Based Solar Cells	6
II.I.I Incoupling of the Photon	7
II.I.II Photon Absorption	8
II.I.III Exciton Formation	10
II.I.IV Exciton Diffusion	12
II.I.V Exciton Dissociation and Charge Separation	13
II.I.VI Charge Transport	16
II.I.VII Charge Collection	19
II.II Conjugated Polymers	20
II.III Device Architectures	27
II.III.I Single Layer Devices	27
II.III.II Bilayer Heterojunction Devices	30
II.III.III Bulk Heterojunction Devices	32
II.III.IV Tandem Solar Cells	37
II.IV Use of Fullerene Derivative in Polymer Solar Cells	38
II.V Conclusions	43
II.VI References	45

III. Experimental Techniques	51
III.I Photovoltaic and Electronic Device Fabrication	51
III.I.I Substrate cutting and ITO PatterningSingle Layer Devices	51
III.I.II Spin Coating of PEDOT:PSS and polymer:fullerene layers	53
III.I.III Cathode Deposition	54
III.I.IV Thermal Annealing	56
III.II Photovoltaic Device Testing and Characterisation	56
III.II.I Current Voltage Measurements	56
III.II.II Series and Shunt Resistance Calculations	61
III.II.III External Quantum Efficiency (EQE) Measurements	62
III.II.IV Temperature Dependent EQE Measurements	66
III.II.V Critical Field Modeling	66
III.III Transmission Electron Microscopy	68
III.III.I The Transmission Electron Microscope	68
III.III.II Sample Preparation	71
III.IV Space Charge Limited Current (SCLC) Mobility Measurements	72
III.IV.II Space Charge Limited Current Mobility Theory	73
III.IV.II Sample Preparation	74
III.IV.III Experiment and Calculation	75
III.V Atomic Force Microscopy (AFM)	75
III.VI Contact Profilometry Measurements of Film Thickness	77
III.VII Optical Surface Profilometry by MicroXAM	79
III.VIII Calculation of Sheet Resistance	80
III.IX Cyclic Voltammetry	84
III.XI UV/Visible Absorption Spectrum	89
III.XII References	90
IV. Revealing the molecular structure of polymer:fullerene composite solar cells by high resolution electron microscopy	91
IV.I Introduction	91
IV.II In situ TEM of the Annealing Process	94
IV.III High Resolution of Pre and Post Anneal Devices	98
IV.IV Investigation of Vertical Segregation	103
IV.V Conclusions	106

IV.VI References	107
IV.VII Appendices.....	110
V. Glycerol Modified PEDOT:PSS in P3HT:PSCBM solar cells	113
V.I Background	113
V.II Hypothesis.....	119
V.III Methods	120
V.IV Results and Discussion	122
V.IV.I UV-Visible Transmission Spectra of Glycerol Modified PEDOT:PSS films	122
V.IV.II Unmasked I-V curves and EQE of Modified Devices.....	124
V.VI.III EQE Spectra.....	126
V.VI.IV Spatially Resolved Current Measurements	130
V.VI.V Masked I-V Curves of Glycerol modified Devices	131
V.VI.VI Surface Topography	133
V.VIII Conclusions	136
V.IX References	137
V.X Appendix	139
VI. Cyclic Voltammetry of fullerene derivatives and Bilayer Devices	141
VI.I Introduction	141
VI.II Fullerene Species of Interest	142
VI.III Cyclic Voltammetry of Fullerene Derivatives	146
VI.IV Bi-layer Solar Cells	153
VI.V Conclusion	159
VI.VI References	160
VII. Bis-ThCBM as an acceptor in P3HT based bulk heterojunction solar cells.....	162
VII.I Introduction	162
VII.II Electronic Properties of bis-ThCBM	164
VII.II.I Electron Mobility of bis-ThCBM	164
VII.III Optimisation of bis-ThCBM solar cells	167
VII.III.I P3HT:bis-ThCBM Devices spin cast from Chlorobenzene	168
VII.III.II P3HT:bis-ThCBM Devices spin cast from ortho-dichlorobenzene (DCB)	173

VII.III.III Origin of the V_{oc} variation in P3HT:bis-ThCBM solar cells	178
VII.III.IV The incorporation of a LiF interfacial cathode layer.....	181
VII.IV Hole Mobility of P3HT:fullerene solar cells determined by SCLC	
Measurements	185
VII.V Critical Field Measurements on P3HT:fullerene solar cells	187
VII.VI Temperature Dependent EQE Experiments on P3HTLbis-ThCBM solar cells	
.....	190
VII.VII Conclusions	193
VII.VIII References	195
VII.VIII Appendices	198
VIII. Conclusions.....	204
VIII.I High Resolution Low Voltage TEM	204
VIII.II Glycerol modified PEDOT:PSS anodes	205
VIII.III Novel Fullerene Derivatives for Enhanced Open Circuit Voltage	206
VIII.IV Future Work	207

List of Abbreviations, Acronyms and Symbols

AFM	Atomic force microscopy
AM1.5	Air mass 1.5
Bis-ThCBM	Bis-thienyl C ₆₁ butyric acid methyl ester
CB	Chlorobenzene
CIGS	Cu(In,Ga)Se ₂
Cu ₂ S	Copper sulfide
C-V	Cyclic voltammetry
DCB	ortho-dichlorobenzene
DMSO	Dimethyl sulfoxide
DS-PEC	Dye-sensitized photoelectrochemical cell
E _E	Exciton energy
E _{EB}	Exciton binding energy
E _F	Fermi energy
E _G	Electrical band gap energy
EQE	External quantum efficiency
F _C	Critical field
FF	Fill factor
FFC	Face centred cubic
FTIR	Fourier transform infrared spectroscopy
G-PEDOT	Glycerol modified PEDOT:PSS
HOMO	Highest occupied molecular orbit
HPLC	High performance liquid chromatopgraphy
HWFE	High work function electrode
IPCE	Incident photon conversion efficiency
IQE	Internal quantum efficiency
I _{sc}	Short circuit current
ITO	Indium tin oxide
J _{sc}	Short circuit current density
LED	Light emitting diode
LiF	Lithium fluoride
LUMO	Lowest unoccupied molecular orbit
LVHRTEM	Low voltage high resolution transmission electron microscopy
LWFE	Low work function electrode
L _D	Exciton diffusion length
NC	Nanocrystal
MDMO-PPV	Poly[2-methyl,5-(3',7'' dimethyloctyloxy)]-p-phenylene vinylene)
MEH-PPV	poly[2-methoxy-5-(2'-ethylhexyloxy)-p-phenylene vinylene]
MIM	Metal Insulator Metal
OLED	organic light emitting diodes
OPV	Organic Based Photovoltaic
PCBM	[6,6]-Phenyl-C ₆₁ butyric acid methyl ester

PCE	Power conversion efficiency
PEDOT:PSS	Poly(3,4-ethylenedioxythiophene) poly(styrenesulfonate)
PEOPT	(poly(3-(4'-(1'',4'',7''-trioxaoctyl)-phenyl)thiophene))
PF	Polyfluorene
PFDTBT	poly(2,7-(9-(2'-ethylhexyl)-9-hexyl-fluorene)- <i>alt</i> -5,5-(4',7'-dithienyl-2',1',3'-benzothiadiazole
PPP	Poly(para-phenylene)
PpyV	poly(p-pyridylvinylene)
PV	Photovoltaic
PPV	Poly(p-phenylene vinylene)
PSS	Polystyrene sulfonate
P3AT	Poly(3-alkylthiophene)
P3HT	Poly(3-hexylthiophene)
RMS	Root mean square
R _S	Series resistance
R _{SH}	Shunt resistance
SA	Secondary additive
SCLC	Space charge limited current
SPS	Sulfonated polystyrene
(<i>t</i> -CH _x)	<i>trans</i> -poly(acetylene)
TCO	Transparent conducting oxide
TEM	Transmission electron microscopy
ThCBM	Thienyl C ₆₁ butyric acid methyl ester
VASE	Variable-angle spectroscopic ellipsometry
V _{oc}	Open circuit voltage
UNSW	University of New South Wales
XRD	X-ray Diffraction
2DFFT	Two dimensional fast fourier transform

I

Introduction

I.I Motivation

The development of abundant, clean and cheap sources of energy is one of society's most urgent priorities and one that is likely to remain a central preoccupation for years to come.

One technology that holds great potential in this regard is photovoltaics; the use of semiconducting materials to produce electricity via the absorption of sunlight. The abundance of the energy source is undeniable, yet the expansion of traditional, inorganic based photovoltaics has always been hampered by an expensive cost-structure that places it at a distinct economic disadvantage compared to traditional options such as coal, gas or hydro-electric.

As such, the fortunes of the photovoltaics industry have always been volatile; dependent on governmental policies and the provision of subsidies in order to achieve economic viability. The roots of this Achilles' heel lie in the high temperature, high vacuum, batch-based production methods used for the panels themselves. While economies of scale have led to significant cost reductions over the last decade, a potentially more transformative approach is to employ polymer-based photovoltaic materials that can leverage the low temperature, ambient pressure, continuous, and low-cost production techniques of the plastics industry.

The efficiency of polymer based solar cells has advanced significantly in recent years with the world record now standing at 7.9% for small area devices. Although this is still significantly below the typical efficiencies reported for conventional solar cells, their theoretical efficiencies are the same, and the organic materials used in polymer based solar cells allow for several key advantages in terms of fabrication and end use.

Polymeric semiconductors have very high absorption coefficients, meaning that only a few hundred nanometres are required in order to absorb most incident light. They are also flexible, and compatible with high throughput, low temperature, and continuous processing methods. As a result, polymer based solar cells have great potential to be cheaply produced at large scale on flexible substrates, which would provide huge advantages over conventional solar cell products. The caveat being that there are significant issues regarding the level of photovoltaic efficiency and long term stability that must first be resolved.

I.II The History of Photovoltaics

The photovoltaic (PV), or more specifically the photoelectrochemical effect was first discovered by Alexandre-Edmond Becquerel in 1839,¹ when he observed a photocurrent produced by silver halide coated, platinum electrodes, illuminated in aqueous solution.² In 1873 and 1876, Smith and Adams first reported the effect of photoconductivity while working with selenium² while

photoconductivity in an organic compound was first noted with Anthracene in 1906 by Pochettino². Research continued throughout the first half of the 20th century and in 1954 Bell Laboratories produced the first inorganic, silicon based solar PV device, with an efficiency of 6%.² This development prompted the New York Times to declare that solar cells will lead to "the realization of harnessing the almost limitless energy of the sun".

Through the 1950s and 1960s silicon PV development was fuelled by the space race and with the 1973 Oil Crisis, silicon based PV development leapt to prominence as a research discipline.

Since then, the history of photovoltaics can be viewed as the development of three overlapping generations of technology. The first generation, initiated by Bell Laboratories in 1954, consists of single-crystal and polycrystalline silicon wafer-based, single-junction devices. This type of device accounts for over 90% of the present day commercial photovoltaic market and the best laboratory based devices exceed efficiencies of 24% under one sun conditions.³

However, despite considerable cost reductions over the years, largely due to improved economies of scale, some researchers believe that the price per watt of first generation photovoltaics will plateau before significantly influencing energy production markets.

This belief led some researchers in the late 1970s to investigate thin film PV technologies that do not require a silicon wafer substrate and can therefore be produced at much lower cost.⁴ In 1980, researchers at the University of Delaware produced the first thin film PV device to exceed

10% efficiency, using $\text{Cu}_2\text{S}/\text{CdS}$ technology. Other second generation, thin film technologies include $\text{Cu}(\text{In,Ga})\text{Se}_2$ (CIGS), multi junction a-Si/a-SiGe and CdS/CdTe cells which have proven to be the most economically effective so far.

Triple junction, $\text{GaInP}/\text{GaInAs}/\text{Ge}$ devices with solar concentration are the most efficient solar cells yet published, exhibiting efficiencies of over 41%⁵.

The concept of third generation PV was first developed by Martin Green at UNSW.⁴ It is based on the premise that incremental improvements of first and second generation technologies will not suffice and that novel technologies will be required to achieve truly cost competitive PV devices. One direction this philosophy can take is the pursuit of very high efficiency devices that have theoretical efficiency limits far in excess of the single junction device ceiling of 31%.⁴ The alternative course is to pursue moderate efficiency at very low cost. It is to this category that organic based, and more specifically, polymer based photovoltaics belong.

Organic photovoltaics (OPVs) have endured a relatively slow development compared to first and second generation technologies. After Pochettino's discovery in 1906, it wasn't until the 1960's that several common dyes, including methylene blue, were found to exhibit semiconductive and then photoconductive properties.² Around this time the PV effect was also observed as a biological phenomenon in molecules such as carotenes, phthalocyanines, and most famous of all, the chlorophylls. However, device efficiencies stubbornly languished around the 0.1% mark and it was not until 1986 that Tang broke the 1% efficiency barrier with a bilayer device of

copper phthalocyanine and a perylene tetracarboxylic derivative.⁶ In 1991, O'Regan and Gratzel reported a dye-sensitized photoelectrochemical cell (DS-PEC) that used a liquid electrolyte and exhibited a power conversion efficiency of 7.1%.⁷ Replacement of the liquid electrolyte with a solid was necessary from a production stand point but at the cost of greatly reducing the device efficiency. Today, the best solid state dye sensitised PV devices exhibit efficiencies of over 5%.⁸ The use of quasi-solid state electrolytes and ionic liquids have helped to push efficiencies even higher to 8.2%.⁹

In 1993, Sariciftci was the first to incorporate C₆₀ into a polymer based PV device¹⁰ after the discovery of ultra-fast electron transfer in C₆₀/polymer blends. Improved performance was achieved with the C₆₀ derivative, PCBM [6,6]-Phenyl-C₆₁ butyric acid methyl ester and today, similar systems, produce the most impressive polymer based PV devices, delivering efficiencies of nearly 8%.¹¹ In 1996 Greenham et al. showed the potential of polymer based PV devices containing quantum confined nanocrystals (NCs) and the last decade has seen the synthesis and incorporation of NCs with increasingly sophisticated morphologies into polymer based PV devices.

II

Review of Organic Photophysics and Chemistry

II.I Photophysics of Polymer Based Solar Cells

There are seven key processes that govern the performance of polymer based PV devices.¹²

While some of these processes are recognizable from conventional photovoltaic theory, others are fundamentally different.¹³

The seven processes are:

1. Incoupling of the photon
2. Photon Absorption
3. Exciton Formation
4. Exciton Diffusion
5. Exciton Dissociation and Charge Separation
6. Charge Transport
7. Charge Collection

The first two processes are optical mechanisms, whereas the last five pertain to the electrical behaviour of the device. As shown in Figure 1, polymer based PV devices typically employ a planar-layered structure consisting of one or more photoactive layers sandwiched between two inorganic electrodes, all mounted on a transparent substrate. The front electrode, generally applied to a transparent substrate, must be transparent itself and is often indium tin oxide (ITO).

The back electrode is a reflective, low work function metal such as aluminium, gold, calcium or magnesium.¹⁴

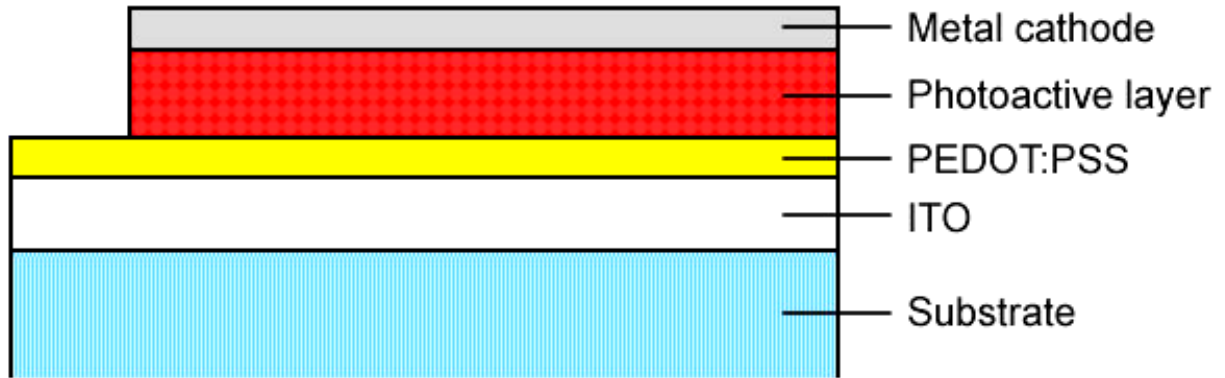


Figure 1. General structure of a polymer based solar cell

II.1.1 Incoupling of the Photon

The transparent substrate is the first layer of the device that incident light encounters and it is often orders of magnitude thicker than the rest of the device combined. Therefore, substrate transparency is highly important and ideally the substrate absorption spectra will exhibit no overlap with the absorption spectra of the photoactive layers. Furthermore reflection losses at the atmosphere/substrate interface should also be minimized. When simplified for normal incidence, the Fresnel equation (Equation 1) shows that the reflectance, R at an interface of two phases is proportional to the square of the difference between the refractive indexes (n) of the two phases. For $n_{\text{substrate}} = n_{\text{glass}} = 1.5$, the reflectance will be $R = 0.04$, but if $n_{\text{substrate}} = 2$, $R = 0.11$. Fused quartz possesses a refractive index of $n_{\text{quartz}} = 1.46$, while the polymer polyethylene which is sometimes used as a substrate has a refractive index of $R = 1.51$.

$$R = \left(\frac{n_{air} - n_{substrate}}{n_{air} + n_{substrate}} \right)^2 \quad (1)$$

It is important to realize that the entire device reflectance depends on all the layers and interfaces in the device, not just the reflectance of the air/substrate interface. Device reflectance as a whole can be minimised by judicious use of surface patterning, coatings, by manipulating layer order and layer thicknesses and by careful choices of the dielectric functions of the layers¹².

II.I.II Photon Absorption

It is desirable to focus as much of the incident radiation as possible on the photoactive layer of an organic PV device. For a bilayer heterojunction device, the photoactive layer of interest typically exists 10nm to 20nm either side of the heterojunction interface. For a bulk heterojunction device, the need to focus incident radiation is less important as excitons can dissociate throughout the bulk of the active layer. The use of a reflective back electrode sets up a standing wave in the optical electrical field E . E is usually defined in terms of its square modulus, $|E|^2$ and at any point in the device $|E|^2$ is a function of the local dielectric function as well as the overall device geometry. By manipulating these variables, including the optical properties of the layers and interfaces, one can manipulate $|E|^2$ and position its maxima at the desired location.

Furthermore, it is desirable that the photoactive components in the device possess absorption coefficients that match the solar spectrum as closely as possible. The conjugated polymers, such

as poly(3-hexylthiophene) (P3HT) used in polymer based PVs tend to absorb well below 650nm but poorly in the red and infrared. As such, their absorption range is relatively narrow compared to the available solar spectrum¹⁴ (Figure 2). Conjugated polymers, and in fact all semiconductors, will not absorb light with energy less than the semiconductor band gap energy (E_g). Recently, researchers have had considerable success creating conjugated polymers with smaller band gaps that enable absorption further into the red and therefore provide a better match to the solar spectrum.^{15,16,17,18,19,20,21,22}

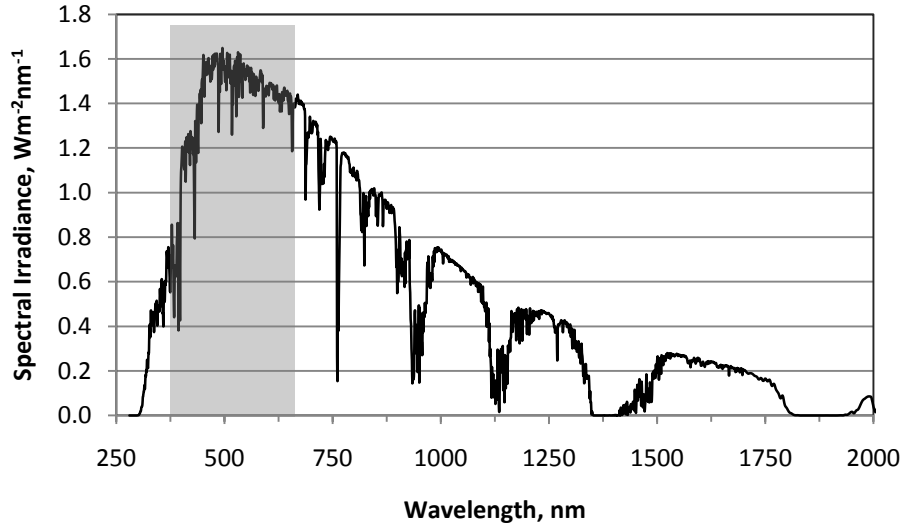


Figure 2. AM1.5 Solar spectrum, showing absorption spectrum of P3HT

Incoupling and Photon Absorption constitute the optical components of polymer based photophysics. A joint efficiency, n_A , the ratio of the number of photons absorbed to the number of photons incident on the device surface, is typically used to quantify their effect.¹²

II.I.III Exciton Formation

There are fundamental differences between the photophysics of conventional semiconductors, such as silicon, and organic semiconductors in terms of charge generation and transport.¹³ In conventional semiconductors, photon absorption produces weakly bound electron hole pairs (excitons) which are easily separated into free charge carriers across the depletion zone. However, in an organic semiconductor, photon absorption produces a strongly bound exciton,¹³ comparable to the Frenkel exciton in solid state physics.¹² This difference arises due to two important factors, one of which is the low relative dielectric constant, ϵ , (also known as the relative permittivity) of conducting polymers. Organic semiconductors typically have a dielectric constant on the order of $\epsilon = 3$, compared to $\epsilon = 10$, for inorganic semiconductors.²³ The dielectric constant quantifies the ability of a material to attenuate the magnitude of an electric field within it. A material with a low dielectric constant, such as an organic semiconductor, is less able to attenuate the electrostatic attraction between hole and an excited electron and hence the charge carriers stay bound in the exciton state. Quantitatively, photo generation of free charge carriers (in conventional semiconductors), or excitons (in organic semiconductors) depends on the square of ϵ .

The second factor is the small Bohr radius, r_B , of charge carriers in organic semiconductors. For semiconducting materials, the Bohr radius of the ground state can be written as

$$r_B = r_0 \epsilon \left(\frac{m_e}{m_{eff}} \right) \quad (1)$$

Where $r_0 = 0.53 \text{ \AA}$, the average distance between the electron wave function and the positively charged nucleus in a ground state hydrogen atom, m_e is the mass of a free electron in vacuum and m_{eff} is the effective mass of the electron in the semiconductor.²⁴ For inorganic semiconductors, m_{eff} is usually less than m_e , whereas in organic semiconductors m_{eff} is typically greater than m_e .

Coulomb's law tells us that the energy of attraction, E , between an electron and hole is equal to:

$$E = \frac{1}{4\pi\epsilon\epsilon_0} \frac{q^2}{r} \quad (2)$$

Where q is the electronic charge, ϵ_0 is the permittivity of free space and r is the distance between the charge carriers. This coulombic attraction is inconsequential if it is less than the average thermal energy of the carriers, or when:

$$E = \frac{q^2}{4\pi\epsilon\epsilon_0} \frac{1}{r_c} = k_B T \quad (3)$$

Where k_B is the Boltzmann constant and r_c is the critical distance between the two charge carriers at which point the two energy terms equate. Equation (4) can be rearranged to give:

$$r_c = \frac{q^2}{4\pi\epsilon\epsilon_0 k_B T} \quad (4)$$

Excitonic behaviour is observed if $r_c > r_B$. As an aside, exciton behaviour is also observed in materials where r_B is greater than the particle radius and is the basis of exciton formation in inorganic nanocrystals.²⁵

Gregg has defined a parameter γ , the ratio of the critical radius to the Bohr radius which highlights the parameters responsible for excitonic semiconductor behaviour. Values of $\gamma > 1$ denote excitonic semiconductor behavior, whereas $\gamma < 1$ indicates a conventional semiconductor:

$$\gamma = \frac{r_c}{r_B} \approx \left(\frac{q^2}{4\pi\epsilon_0 k_B r_0 m_e} \right) \left(\frac{m_{eff}}{\epsilon^2 T} \right) \quad (5)$$

This equation is a rough approximation for a number of reasons²⁵ and therefore engenders a high degree of uncertainty for semiconductors where γ nears 1. However such instances are rare with $\gamma \gg 1$ for the vast majority of organic semiconductors.

The energy possessed by the exciton, E_E , is slightly less than the electrical band gap energy, E_G , of the semiconducting polymer i.e. the energy required to produce separated charge carriers, due to the exciton binding energy, E_{EB} (see Figure 3). Therefore it can be written that:

$$E_G = E_E + E_{EB} \quad (6)$$

In most cases the exciton binding energy is of the order of 0.2 – 0.4 eV^{26,27,28} depending on the polymer.

II.I.IV Exciton Diffusion

Excitons are a charge neutral, metastable species. As such, they move by diffusion via intra-chain or inter-chain energy transfer or “hopping,” including Förster energy transfer.²⁹ The exciton

diffusion length, L_D , is defined as the average distance an exciton travels before its extinction and is typically in the range of 5nm – 20nm for organic semiconductors.^{30,31} L_D is affected by the degree of disorder in the material, the density of trapping sites and the dielectric environment.^{12,30} A number of events can mark the extinction of an exciton. Undesirable extinction events include; radiative decay, whereby the electron and hole recombine and release a photon; vibronic decay, whereby recombination releases a series of phonons, thermal decay where the energy released in recombination is released as heat, or dissociation into a trapped state. The desired path is the dissociation of the exciton into free charge carriers at a type-II heterojunction (see Figure 3).

II.I.V Exciton Dissociation and Charge Separation

At a dissociation site the electron and hole are electronically separated and subsequently free to move independently of one another. A type-II heterojunction, also known as a donor-acceptor interface, can consist of any two materials with energy band offsets as shown in Figure 3. In polymer based PV devices the acceptor is typically a polymer. The donor may be another polymer, C_{60} (or a C_{60} derivative) or an inorganic nanocrystal (NC).

The thermodynamic requirement for exciton dissociation is that the difference in potential energy (i.e. $LUMO_{Donor} - LUMO_{acceptor}$ or $HOMO_{Donor} - HOMO_{Acceptor}$), at the heterojunction must be greater than the binding energy of the exciton.

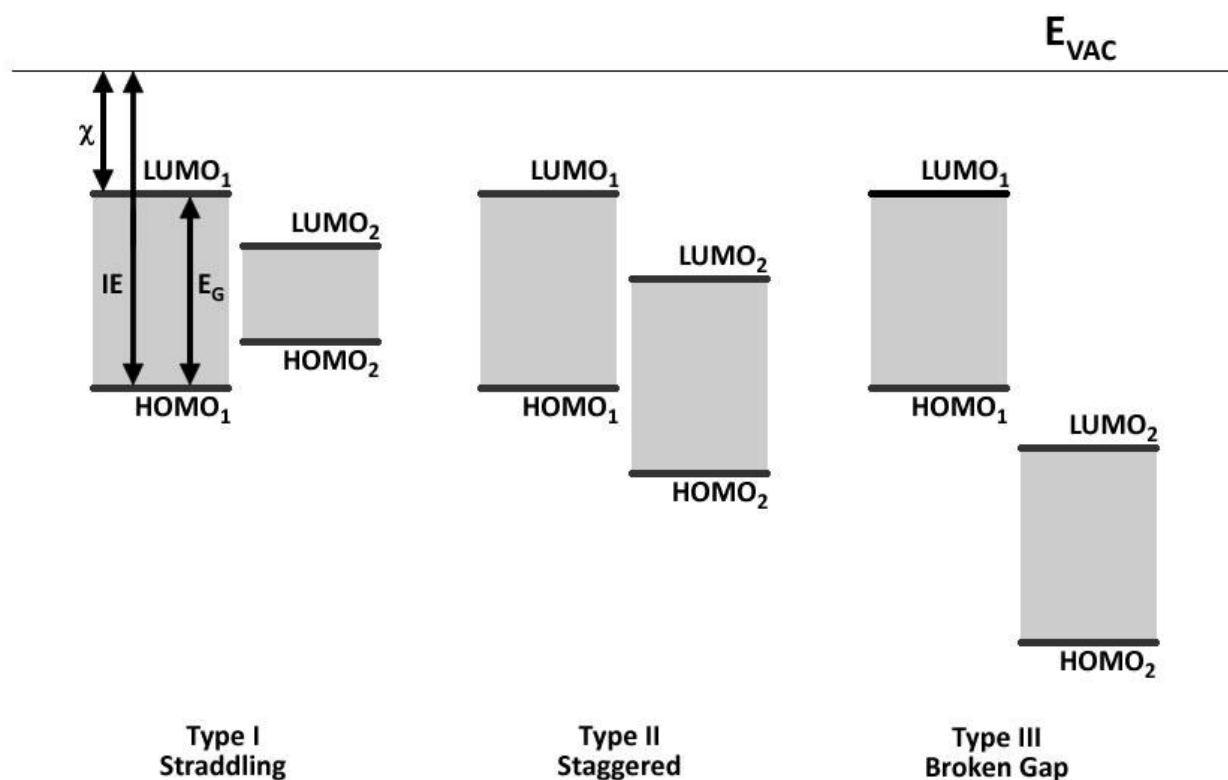


Figure 3. Schematic Representation of a Type I, Type II and Type III heterojunctions. Included are the Highest Occupied Molecular Orbital (HOMO), Lowest Unoccupied Molecular Orbital (LUMO), electron affinity (χ), Ionisation Energy (IE) and Electrical Band gap Energy (E_G).

When an exciton dissociates, one carrier must remain in the original phase, in an available potential energy level. This level defines the potential energy of the injected carrier. For example, when an exciton in the donor material injects an electron into the acceptor, the initial potential of the electron is an exciton energy above the acceptor valence band; and when an exciton in the acceptor material injects a hole into donor, the initial potential of the hole is an exciton energy below the donor conduction band. In both cases the injected carriers relax to the band edge potentials of the new phase, i.e. the electron relaxes to the acceptor conduction band

potential, and the hole relaxes to the donor valence band potential. This relaxation, known as thermalisation, is a loss mechanism and manifests as the emission of heat.

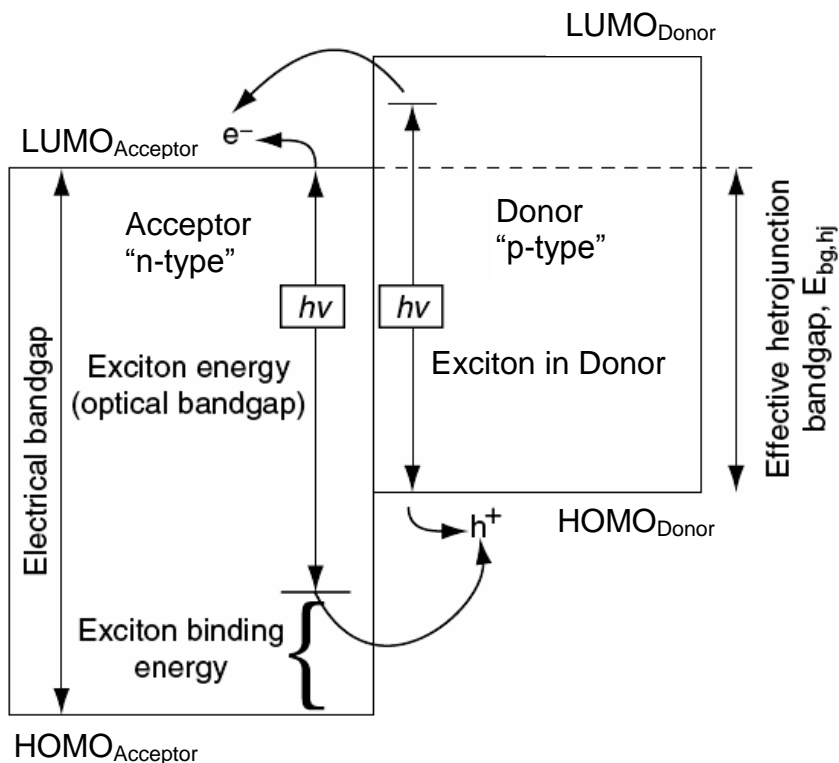


Figure 4. Type II Heterojunction where the Lowest Unoccupied Molecular Orbit (LUMO) and Highest Occupied Molecular Orbit (HOMO) of the Acceptor material lie below the respective LUMO and HOMO of the Donor.³²

Mechanisms that counteract dissociation include geminate recombination, which is the process whereby an electron and a hole from the same exciton recombine, emitting light and/or heat, and non-geminate bimolecular recombination, where an electron and a hole dissociated from different excitons recombine¹².

In recent years, geminate re-combination has been identified as a major loss mechanism in polymer:polymer and polymer:fullerene solar cells.^{33,34} Although exciton dissociation across a type 2 heterojunction can be exceedingly efficient, due to the relatively low dielectric constant of the organic materials, the subsequently formed geminate electron-hole pair (polaron pair) is strongly bound by coulomb interaction, with a binding energy on the order of several tenths of an electron volt.³³ Models of PPV:PCBM based solar cells suggest that as many as 40% of the photogenerated polaron pairs fail to separate into free charge carriers³³ and the linear dependence of net photo current on incident light intensity indicates that geminate recombination is the dominant loss mechanism for a wide range of excitonic solar cells.³⁴

II.I.VI Charge Transport

Once dissociated from an exciton, the free charge carriers must reach their respective electrodes to contribute to the photocurrent. Holes must reach the high work function electrode (HWFE), typically Indium Tin Oxide (ITO) and electrons must reach the low work function electrode (LWFE), typically aluminium.

Dissociation creates a concentration of holes in one chemical phase, and a concentration of electrons in the other chemical phase. This spatial segregation of photogenerated charge carriers does not occur in inorganic PV devices and results in a powerful driving force for carrier separation that is unique to organic PV devices.

Let us consider E , the electrochemical potential, which can be viewed as the sum of two components; the electrical potential, U , and the chemical potential, μ .

$$E = U + \mu \quad (7)$$

The spatial gradient of a potential energy is a force and in a PV device, ∇E is the primary force that drives the charge carrier fluxes²⁵. In equilibrium devices, E represents the Fermi level, E_F . When a device is not in equilibrium, electrons and holes require independent expressions of their respective Fermi levels, E_{Fn} and E_{Fp} . The spatial gradients of these “quasi” Fermi levels, ∇E_{Fn} and ∇E_{Fp} , are the forces that drive the electron and hole fluxes within a device and each is made up of the two quasi-thermodynamic forces ∇U and $\nabla \mu$.

The general kinetic expression for the one dimensional current density of electrons through a device is:

$$J_n(x) = n(x)\mu_n \{\nabla U(x) + \nabla \mu(x)\} = n(x)\mu_n \nabla E_{Fn}(x) \quad (8)$$

Where $n(x)$ is the electron density and μ_n is the electron mobility. Equation 9 can similarly be written for the hole current density. Together these two terms determine the magnitude of the electron flux, while the sum $\nabla U(x) + \nabla \mu(x)$ controls its direction. It can be seen from equation (9) that $\nabla U(x)$ and $\nabla \mu(x)$ are equivalent forces. In inorganic semiconductors, $\nabla \mu(x)$ is insignificant because free charge carriers are generated throughout the bulk and high carrier mobilities allow charge carriers to quickly reduce any ‘unevenness’ in the spatial distribution of charges. $\nabla U(x)$, provided by the offset between the electrode work functions, dominates and determines the flux directions.

In organic PV devices, the spatial separation of charge carriers that occurs during dissociation produces a significant carrier concentration gradient (Figure 5), proportional to $\nabla\mu_{hv}$ (the chemical potential energy gradient under illumination). Furthermore, this gradient is accentuated by the often low equilibrium charge carrier density in the bulk and $\nabla\mu_{hv}$ can be the dominant driving force in organic PV devices²⁵. This is most obvious in functioning bilayer organic devices with matching electrodes, i.e. where $\nabla U = 0$.

In bulk heterojunction devices, the effect of $\nabla\mu_{hv}$ is less ordered due to the highly complicated heterojunction interface. However, it can still be expected to play an important role in charge separation.

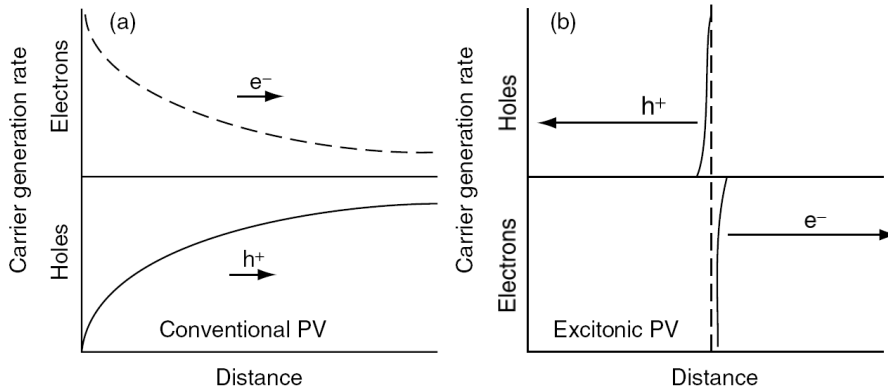


Figure 5. With illumination from the left hand side of the diagram, charge carriers are generated in a Beer's Law Distribution in an inorganic PV devices (a). As such $\nabla\mu_{hv}$ (represented by arrows), drives both carrier types in the same direction. However, ∇U (not shown) is dominant and acts to drive charges in opposite directions towards their respective electrodes. In organic PV devices $\nabla\mu_{hv}$ drives electrons and holes in opposite directions away from the heterojunction and can be the dominant driving force²⁵.

Returning to Equation 9, it was mentioned that the charge mobility, μ_n or μ_p , is a key factor in determining the magnitude of the carrier fluxes. The charge mobility of conjugated polymers is generally low, ranging between $\mu \sim 10^{-5}$ to $10^0 \text{ cm}^2/\text{Vs}$ ³⁵, and far below those found for inorganic semiconductors such as Si ($\mu \sim 10$ to $1000 \text{ cm}^2/\text{Vs}$ doping dependant) ³⁶. Furthermore, conjugated polymers possess hole mobilities that are significantly larger than their electron mobilities. As such, hole transport occurs along the polymer backbones while electron transport occurs within the acceptor phase.

II.I.VII Charge Collection

The final barrier that a charge carrier faces is transfer from the edge of the active layer into its electrode. In an ideal device, the Fermi level of the LWFE would match the acceptor LUMO level, and the Fermi Level of the HWFE would match the donor HOMO level. Due to material constraints, this perfect arrangement is rarely realised. In P3HT:fullerene devices, the use of the conducting polymer poly(3,4-ethylenedioxythiophene) poly(styrenesulfonate) (PEDOT:PSS) helps to align the anode work function with the HOMO of P3HT (Figure 1. General structure of a polymer based solar cell). At the cathode, it is believed that the electrode potential of low work function metals such as Aluminium, pin to the fullerene LUMO level, facilitating an Ohmic contact. ^{37,38}

II.II Conjugated Polymers

In 1977 Shirikawa, MacDiarmid and Heeger reported that doping films of a conjugated polymer, polyacetylene, with iodine increased the film conductivity by over seven orders of magnitude ³⁹. With this discovery, the field of Conducting Polymers was born, and in 2000 the authors shared the Nobel Prize in Chemistry for this work.

Conjugated polymers consist of repeated functional units connected along a backbone of alternating single (σ -bond) and double (σ -bond plus a π -bond) carbon-carbon bonds. The σ - bond is formed as the carbon atoms are sp^2 hybridised. This configuration leaves the p_z orbital free to form additional π -orbitals, with unit angular momentum about the bond axis, with overlapping p_z electrons in adjacent atoms. The electrons in these overlapping orbitals form p -electron clouds, delocalized over the conjugation length of the polymer (Figure 6).

In accordance with the Pauli Exclusion Principle, overlapping p_z orbitals actually form two distinct orbitals of separate energy; the bonding π -orbital and the antibonding π^* -orbital. The difference in energy between the π -orbital and the π^* -orbital constitutes the polymer's electronic band gap. As a general rule of thumb, the longer the conjugation length of the polymer, the smaller the electronic band gap.

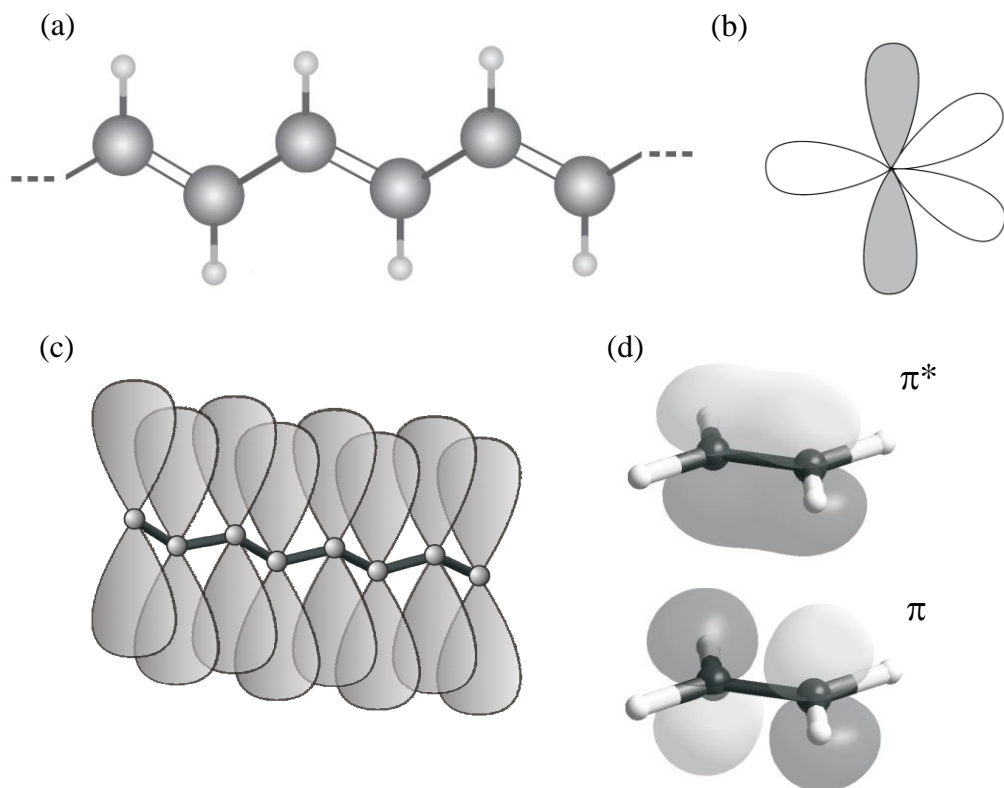


Figure 6. (a) Structure of polyacetylene, showing carbon backbone of alternating double and single bond ⁴⁰. (b) sp^2 hybrid orbitals (σ -bonds) lie in a plane with an angle of 120° between them. The π -orbitals (shaded) lie orthogonal to the plane of the σ -bonds ⁴⁰. (c) Schematic representation of p_z orbital overlap in a conjugated segment of the polymer ²³. (d) Bonding π and antibonding π^* orbitals on the primary conjugated molecule ethylene ²³.

However, the semi conducting polymers are not ideal conjugated systems. The absence of long range three dimensional order, different intramolecular and intermolecular interactions, local structural disorder such as twisting and kinking of the polymer chains, discontinuities between amorphous and crystalline regions, and chemical impurities cause fragmentation in the polymer conjugation length.

In fact, at least in the case of Poly(p-phenylene vinylene) (PPV), a significant amount of research suggests that conjugated polymers can be regarded as arrays of chromophores consisting of fully

conjugated segments of polymer chains of 6- 10 monomeric units. It has been found that the optical transitions of these segments are similar to those of oligomeric model compounds of comparable length and that the global optical and electronic properties of the polymer are determined by the ensemble of these conjugated segments^{41,42}.

The variation in conjugation length causes spread in the π and π^* electronic energy levels (Figure 7) which means that, unlike inorganic semiconductors, organic semiconductors cannot be described by band theory models, i.e. they cannot be described by delocalised valence and conduction bands formed by π and π^* orbitals respectively.

The spread in energy levels of the π -orbitals (also known as the Highest Occupied Molecular Orbit or HOMO) and π^* -orbitals (also known as the Lowest Unoccupied Molecular Orbit or LUMO) can be approximated by a Gaussian distribution. (Figure 7b). For most conjugated polymers the gap between the HOMO and LUMO levels is in the range 1.5-3 eV.

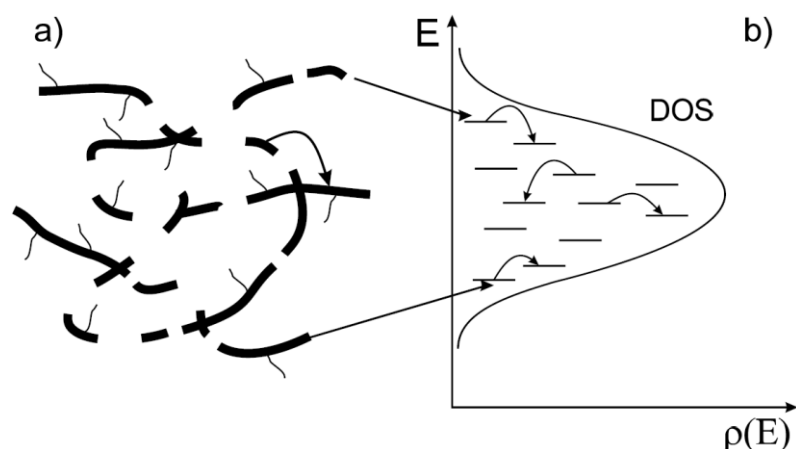


Figure 7. (a) The disorder of a conjugated polymer, shown as an array of conjugated segments. (b) Energy distribution of the localized states, approximated by the Gaussian. Exciton hopping is also shown (arrows) ²³.

The discovery of conjugated polymers heralded a class of materials with the potential for tunable optoelectronic properties and low cost, solution based processing. However, nearly all the straight chain conjugated polymers are insoluble, greatly hindering their processability ⁴³. The addition of side groups, most commonly long alkyl or alkoxy groups, greatly increases polymer solubility ^{44,45,46}.

There are an increasing number of such modified conjugated polymers now available for use in organic photovoltaics. One of the first to be used was poly[2-methoxy-5-(2'-ethylhexyloxy)-p-phenylene vinylene] (MEH-PPV), following its successful application in organic light emitting diodes (OLEDs). Poly(3-hexylthiophene) (P3HT) is another commonly used polymer, especially in conjunction with PCBM. Its smaller band gap, improved charge mobility, high regioregularity and more crystalline structure make it a more promising material than MEH-PPV. A number of derivatives of polyfluorene (PF) and poly(para-phenylene) (PPPs) have also been investigated ⁴⁷.

It is only relatively recently that researchers have started working on developing polymers specifically for OPV application⁴⁸.

The main design goal has been to produce polymers with smaller band gaps while still maintaining a high absorption coefficient and suitable HOMO and LUMO levels in order to facilitate exciton dissociation with a fullerene derivative⁴⁹.

The first approach that emerged was to broaden the absorption range of known polymers. For example, bi(thienylenevinylene) substituted polythiophenes,⁵⁰ whereby 2,5-bis(tributylstannyl)thiophene is conjugated to a polythiophene backbone, was shown to improve absorption into the UV and when mixed with PCBM it outperformed P3TH:PCBM reference cells.

A second, and more fruitful approach has been the development of completely new 'low bandgap' polymers, which generally refers to any polymer with a band-gap lower than P3HT (1.9 eV). Most commonly, researchers have used the donor acceptor approach, in which the polymer backbone consists of alternating electron-rich and electron-poor units.⁵¹ To date, the best examples of this approach use benzothiadiazole as the acceptor, in conjunction with a range of donor groups. Band gaps as low as 1.5 eV have been reported,²² with efficiencies ranging as high as 6.1%.^{16,18,22,52}

Most recently, researchers have sought to optimize not only the polymer band gap, but also the polymer HOMO level, in order to optimize the open circuit voltage. Benzodithiophene based

polymers have been shown to be highly tunable in both band gap and HOMO level,^{19,20} with efficiencies as high as 6.8% achieved⁵³ – the highest efficiency for a polymer:fullerene solar cell published in the academic literature to date. Figure 8 gives a summary of the major conjugated polymers applied in photovoltaic devices.

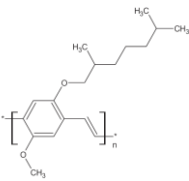
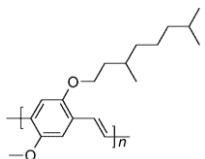
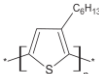
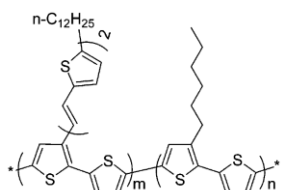
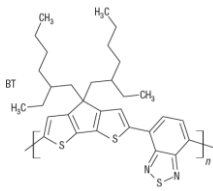
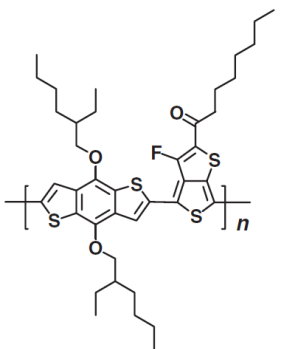
Structure	Name	HOMO, eV	Band gap, eV
	Poly[(2-methoxy-5-[3,7-dimethyloctyloxy])paraphenylene vinylene] (MEH-PPV)	-5.26 ⁵⁴	2.2 ⁴⁹
	Poly[2-methoxy-5-(3',7'-dimethyloctyloxy)-1,4-phenylenevinylene] (MDMO-PPV)	5.3 ⁵⁵	2.3 eV ⁵⁶
	Poly(3-hexylthiophene) (P3HT)	-5.01 ⁵⁴	1.9 ⁴⁹
	bi(thienylenevinylene) substituted poly(3-hexylthiophene)	4.95 ⁵⁰	1.99 ⁵⁰
	poly[2,6-(4,4-bis-(2-ethylhexyl)-4H-cyclopenta[2,1-b;3,4-b]-dithiophene)-alt-4,7-(2,1,3-benzothiadiazole)] (PCPDTBT)	-5 (approx) ²²	1.46 ²²
	poly[N-900-hepta-decanyl-2,7-carbazole-alt-5,5-(40,70-di-2-thienyl-20,10,30-benzothiadiazole)PCDTBT	-5.5 eV ¹⁸	1.9 ¹⁸
	poly[4,8-bis-substituted-benzo[1,2-b:4,5-b']dithiophene-2,6-diyl-alt-4-substituted-thieno[3,4-b]thiophene-2,6-diyl] (PBDTTT-CF)	-5.22 ⁵³	1.77 ⁵³

Figure 8. A selection of conjugated polymers used in organic photovoltaics.

II.III Device Architectures

II.III.I Single Layer Devices

The first simple, polymer based PV devices were reported by Weinberger in 1982. They consisted of a layer of *trans*-poly(acetylene) ($t\text{-CH}_x$) sandwiched between electrodes of graphite and aluminium⁵⁷. The devices were intrinsically inefficient as charge photogeneration can only take place in a thin layer near the polymer/electrode interface. Poor exciton dissociation and excessive geminate recombination also limited performance. By 1984, similar devices reported by Kanicki and Fedorko achieved a PCE of only 0.1% under a 50W/m^2 xenon light, despite a respectable V_{OC} of 0.65V⁵⁸.

Over the following ten years, little progress was made with single layer devices despite the application of a number of different polymers. A number of polythiophene derivatives were investigated^{59,60}, with Fang et al. reporting a PCE $\sim 0.01\%$ for poly(3-butylthiophene) (P3BT) in 1982⁶⁰. In 1994 Poly(p-phenylene vinylene) (PPV) and Poly[(2-methyloxy-5-[3,7-dimethyloctyloxy]]paraphenylene vinylene] (MEH-PPV) based devices with ITO and metal electrodes were developed by groups at Cambridge⁶¹ and Santa Barbara⁶² respectively (Figure 9). These devices exhibited PCE $\approx 0.03\%$ at low light levels⁶².

Despite the intrinsic inefficiency of these single layer devices, they are well explained by the Metal-Insulator-Metal (MIM) model, which offers the simplest model for understanding the rectifying behaviour of an intrinsic semiconductor device. In Figure 10 such a device is shown for

four different conditions. In Figure 10a there is no applied voltage, a situation known as the short circuit condition. In the dark, there is no current flowing and the built-in electric field is evident, formed by the difference between the work functions of the electrodes. Under illumination, separated charge carriers can drift in this electric field towards their respective contacts. The device is producing electricity and the device functions as a solar cell. Figure 10b shows the device in the open circuit, or 'flat band' condition. The applied voltage now balances the inbuilt electric field and there is no net driving force for the charge carriers. The current is therefore zero. In Figure 10c, the device is shown in 'reverse bias'. Under illumination the applied electric field aids the inbuilt electric field in driving charge carriers to their respective electrodes. The device is consuming energy and working as a photodetector. In Figure 10d, the device is shown in 'forward bias'. Here an applied voltage greater than the V_{oc} is used to inject charge carriers into the polymer. If these charges can combine radiatively, the device works as a light emitting diode (LED).

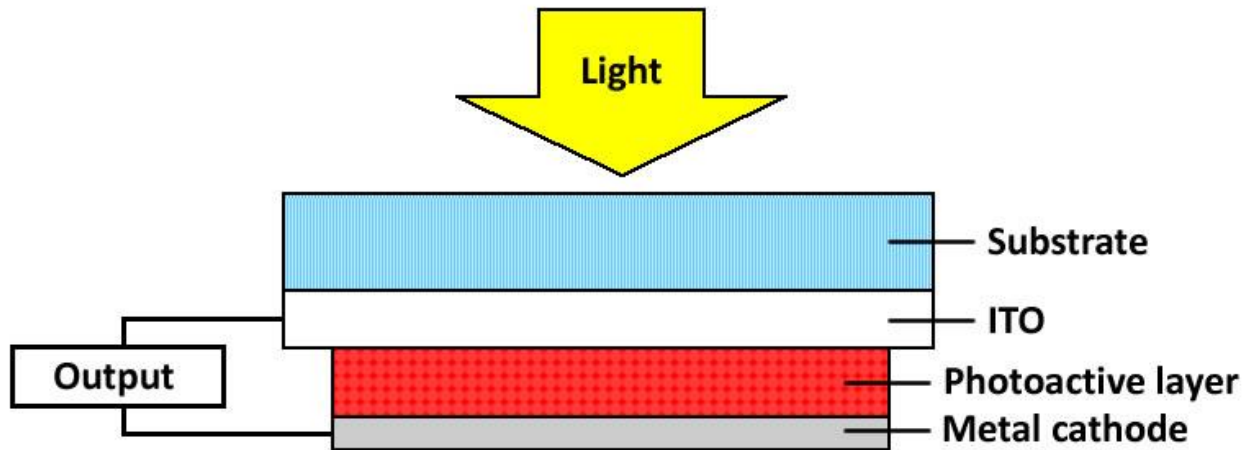


Figure 9. A typical single layer organic PV device consisting of a glass substrate, transparent ITO anode, polymer layer and metallic back electrode ².

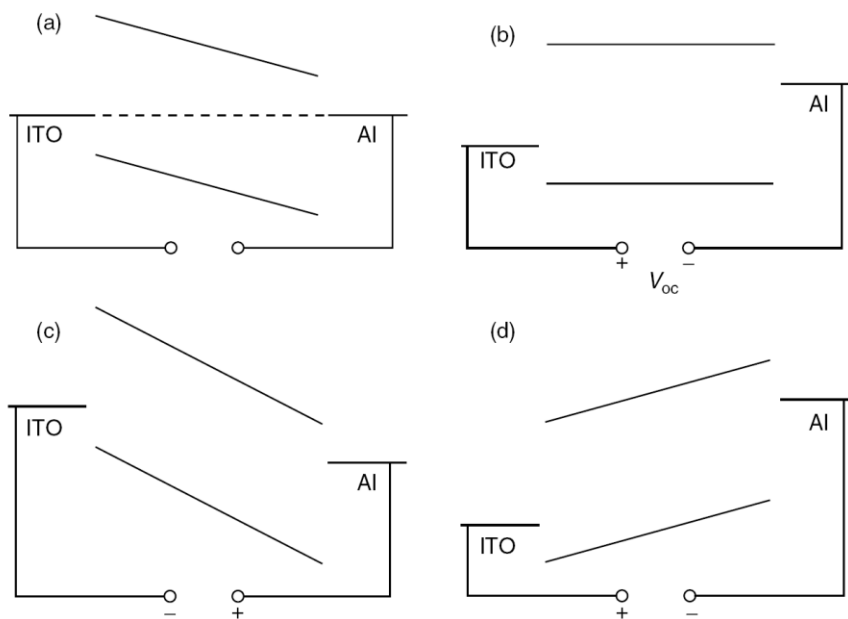


Figure 10. Single Layer Polymer PV device with ITO and Al electrodes shown at (a) short circuit, (b) open circuit, (c) reverse bias, (d) forward-bias

II.III.II Bilayer Heterojunction Devices

In 1979 Tang filed a patent ⁶³ on his ability to produce a PCE \approx 1% in a bilayer device of copper phthalocyanine and a perylene tetracarboxylic derivative ⁶. His work was not published in the academic literature until 1986, but even then it marked a significant step in the development of organic photovoltaics. As mentioned previously, if the interface of two materials form a suitable type-II heterojunction, an exciton bound electron in the donor material can dissociate across the interface from the $\text{LUMO}_{\text{Donor}}$ into the $\text{LUMO}_{\text{acceptor}}$. Similarly an exciton bound hole in the acceptor can dissociate across the interface from the $\text{HOMO}_{\text{acceptor}}$ to the $\text{HOMO}_{\text{donor}}$. Dissociation at such an interface can be far more efficient than the polymer/electrode interface dissociation of a single layer device. Furthermore, bilayer devices provide the advantage of single charge carrier transport after the dissociation event. This greatly reduces the chances of non-germinate recombination.

Bilayer devices incorporating conjugated polymers didn't appear in the literature until 1993 ¹⁰ and were preceded by some very important work conducted independently by Sariciftci et al. and Yoshino et al. on the photophysics of mixtures of C_{60} and conjugated polymers ^{64,65,66,67,68}. C_{60} is a strong electron acceptor with a three-fold degenerate LUMO of accepting six electrons ⁶⁹. The work by Sariciftci et al. revealed an ultra-fast, reversible, metastable photo-induced electron transfer from conjugated polymers onto C_{60} in solid films. The work by Yoshino et al. on mixtures of C_{60} and Poly(3-alkylthiophene) (P3AT) showed the phenomenon was not restricted to MEH-PPV.

The first device, published by Sariciftci et al. in 1993, incorporated a layer of C_{60} vacuum sublimed onto a spin coated layer of MEH-PVV with electrodes of Aluminium and Gold ¹⁰. The device exhibited a FF of 0.48 and a PCE of 0.04% under monochromatic (514.5nm) illumination at $1\text{mW}/\text{cm}^2$. Most importantly, the photocurrent increased by a factor of 20 upon the application of the C_{60} layer. Later that same year, Morita et al. presented similar results for devices based on P3AT ⁷⁰.

In 1996 Halls et al. published a study of PPV/ C_{60} devices that exhibited a V_{OC} approaching 0.9V and an EQE of 9% under monochromatic illumination (492nm) at $0.7\text{mW}/\text{cm}^2$. More importantly, the authors estimated an exciton dissociation length of 6-8nm and investigated the importance of layer thickness on device optimisation ⁷¹.

It became evident that controlling the layer thicknesses was very important for controlling the distribution of the optical-electric field within devices, with the desired result being to maximise the field at the heterojunction. In 1999 Pettersson et al. modelled the optical field density through a (poly(3-(4'-(1'',4'',7''-trioxaoctyl)-phenyl)thiophene)) (PEOPT)/ C_{60} device ⁷². They reported exciton diffusion lengths consistent with Halls and reported an optimised device with a PCE of 1.7% under monochromatic (460nm) illumination at $15\mu\text{W}/\text{cm}^2$ ⁷³.

In 2003, Durstock et al. used electrostatic self-assembly to precisely control the layer thicknesses in PPV/SPS/ $C_{60}^+C_{60}^-$ devices (SPS stands for sulfonated polystyrene) with interfacial layers of PPV/ C_{60}^- .

Polymer/polymer bilayer devices have also been investigated by some researchers but face the additional challenge of selecting a solvent for the top layer that will not dissolve the first layer when the top layer is spin coated. In 1999 Tada et al. reported a device consisting of a poly(p-pyridylvinylene) (PpyV) acceptor layer and a poly(3-hexylthiophene) (P3HT) donor layer ⁷⁴.

II.III.III Bulk Heterojunction Devices

Although it is clear that the bilayer device architecture overcomes many of the weaknesses of the single layer device, it still suffers from considerable drawbacks itself. With exciton dissociation most efficient at the heterojunction interface and the exciton diffusion length limited to around 10nm, the light harvesting area of the device is limited to approximately 20nm. For most conjugated polymers this is only one fifth of the thickness required to absorb most of the incident radiation at sunlight intensities ². The solution was the bulk heterojunction, where donor and acceptor materials are intimately mixed throughout the active layer on the scale of the exciton diffusion length.

The first polymer based bulk heterojunction was published in 1994 by Yu et al. It consisted of a 10:1 solution of MEH-PPV and C₆₀ in xylene spun cast onto an ITO covered glass substrate with a Calcium back electrode Under 2.8mW/cm² illumination at 500 nm, the current density $J_{SC} = 15.3$ mA/cm², corresponding to an EQE of roughly 1.3%, and $V_{OC} = 0.8V$. This represented an order of magnitude improvement over neat MEH-PPV devices. In 1996 Kohler et al. ⁷⁵ used a similar approach with devices containing a mixture of the polymer Pt-Pt-poly-yne with 7wt% C₆₀ and an Al back contact. An EQE of 1.6% was observed.

These bulk heterojunction devices improved upon the polymer/C₆₀ bilayer devices but still fell short. As charge photogeneration appeared to be highly efficient in even low C₆₀ weight percent mixtures, it was realized that charge transport was the limiting process in these new devices. Specifically, the concentration of C₆₀ was not high enough to create a continuous percolation network by which the separated electrons could access the metallic electrode. The concentration of C₆₀ was limited by the molecules' tendency to crystallize during spin coating and its rather low solubility in the organic solvents used for spin coating polymer films.

In 1995, the solution to this dilemma appeared in the field of fullerene chemistry when Hummelen et al.⁷⁶ synthesised a number C₆₀-derivatives with increased solubility.

Yu et al. repeated their fabrication procedure using a methanofullerene derivative 1-(3-methoxycarbonyl)-propyl-1-phenyl-(6,6)C₆₁ or [6,6]-PCBM, which allowed the fabrication of films with up to 80wt% PCBM, equating to roughly one fullerene per polymer repeat unit⁷⁷. They reported devices with $V_{OC} = 0.82$, EQE = 29% and PCE = 2.9% under monochromatic illumination (430nm) at 20mW/cm².

A paper by the Sariciftci group in 2000 further emphasized the importance of the bulk heterojunction morphology on device performance⁷⁸. In a (poly)[2-methyl,5-(3',7'' dimethyloctyloxy)]-p-phenylene vinylene) (MDMO-PPV)/PCBM device, just changing the solvent used to spin cast the active layer from Toluene to Chlorobenzene was enough to increase the device efficiency by nearly 300%, yielding an PCE = 2.5% at AM1.5 conditions. The improvement

was correlated with reduced segregation in the MDMO-PPV/PCBM mixture via AFM images of the device surface morphology.

Further studies in the group focusing on the inclusion of very thin ($<15\text{\AA}$ thick) layer of LiF at the interface between the active layer and the metallic electrode further increased the device efficiency to 3.3% under AM1.5 conditions ⁷⁹. The authors believed that the formation of a dipole moment across the interface, due to either orientation of the LiF or chemical reactions leading to charge transfer across the interface, was the mechanism most likely responsible for the enhancement.

In 2002, Munter et al. showed that the route of polymer synthesis can also be exploited to improve the efficiency of polymer/PCBM bulk heterojunction devices. Specifically, for the synthesis of MDMO-PPV, the sulphonyl synthesis route produced a polymer with reduced levels of defects that led to devices with PCE $\sim 2.9\%$. In comparison, devices made with polymer synthesised via the previously favoured gilch route achieved a PCE of only 2.5% ⁸⁰.

A number of other polymers have been used in polymer/PCBM bulk heterojunction devices. In 2003, polyfluorenes were the latest development of new materials for polymer light emitting diodes (PLED). Their high mobility, stability and the ability to form a liquid crystal state at high temperatures also made them an interesting prospect for PV applications. Svensson et al. ⁸¹ reported a device using a polyfluorene copolymer, poly(2,7-(9-(2'-ethylhexyl)-9-hexyl-fluorene)-*alt*-5,5-(4',7'-dithienyl-2',1',3'-benzothiadiazole (PFDTBT). They consisted of an active layer of

PFDTBT and PCBM in a ratio of 1:4, with an ITO cathode and an anode of LiF and Al. An EQE ~ 40% and PCE = 2.2% was achieved under AM1.5 conditions. Of most interest was the relatively high V_{oc} (1.04V).

Another polymer that has risen to prominence in the last 4 years is poly(3-hexylthiophene) (P3HT) due to its smaller band gap and improved charge transport characteristics. In 2004 Schilinsky et al.⁸² reported devices of P3HT:PCBM in a ratio of 1:3 atop a layer of PEDOT:PSS coated ITO with an anode of calcium capped silver. An EQE of 70% was reported at 530nm. Under AM1.5 conditions a relatively high I_{sc} was reported (8.7mA/cm²). This was attributed to P3HTs better alignment with the solar spectrum. However, a V_{oc} of only 0.58V was reported. This still gave a very respectable PCE of 2.8%. The authors also proved, via intensity dependant photocurrent measurements, that the rate of bimolecular recombination in the device was negligible. They speculated that the minimisation of optical losses within the device and substrate may realise EQEs in excess of 90%.

Recent research has focused on heat treatments of the P3HT/PCBM layer to optimise the morphology of the bulk heterojunction by improving the bulk heterojunction morphology and crystallinity of the P3HT phase. Impressive results have been achieved. In 2005 Heeger et al.⁸³ reported a relatively simple device of ITO/PEDOT:PSS/P3HT:PCBM/Al with PCE = 5% under AM1.5. The key factor was the relatively low P3HT:PCBM ratio of 1:0.8 which prevented the formation of overgrown PCBM crystals during the annealing step. Annealing at 150°C produced a

thermally stable interpenetrating donor-acceptor network that retained its PV properties even after annealing times of several hours.

Later that year Reyes-Reyes et al.⁸⁴ reported P3HT/PCBM devices with an LiF and Al anode with PCE = 5.2%. These devices were heat treated at 155°C for only 3 minutes and achieved a slightly higher V_{OC} (0.66V) than the Heeger device (0.6V). Furthermore, the P3HT:PCBM ratio was even lower, at 1:0.6. Reyes-Reyes et al. opined that the thermal treatment facilitates the existence of a pseudofluidic state in which P3HT and PCBM are allowed to rearrange into crystalline nano-domains and thereby providing a very sensitive method of controlling the charge mobility.

Subsequently, the bulk heterojunction architecture has been seen as the design of choice for high efficiency polymer:fullerene solar cells, with most research focusing on improving the photoactive materials used within it. Developments in conjugated polymer synthesis has been discussed above while innovations regarding fullerene derivatives will be discussed in Section IV below.

Efforts to optimise the optical field within bulk heterojunctions have not attracted a huge amount of attention so far. However, in 1995 Geens et al.⁸⁵ did report that sandblasting the glass substrates of MEH-PPV/C₆₀ bilayer devices improved I_{SC} from 5.5mA/cm² to 6.3mA/cm². In 2009, Park et al.¹⁸ introduced a TiO_x spacer layer between the photoactive layer and the metal cathode of a PCDTBT:PC₇₁BM solar cell. The spacer is believed to optimise the light intensity

distribution within the cell, act as a hole blocking layer and to protect the photoactive layer during cathode deposition.

II.III.IV Tandem Solar Cells

The development of the TiO_x layer also facilitated the invention of the tandem bulk heterojunction solar cells of which there have been two notable reports to date.^{86,87} In 2007 Kim et al. reported a tandem device consisting of one P3HT:PC71BM sub-cell and one PCPDTBT:PC₆₁BM sub-cell. A layer of TiO_x was spin cast between the sub-cells to act as a recombination centre and to allow one sub-cell to be spin cast on top of the other, without dissolving the underlying cell. The optimised tandem cell proved to convert photons out to 900nm and obtained an open circuit voltage of 1.24V and an overall efficiency of 6.5%. Interestingly, the most efficient device, due to the lower efficiency of the PCPDTBT sub-cell, was achieved with an inverted structure, with the larger bandgap P3HT sub-cell at the back of the device.

In 2009, Sista et al. published a similar device incorporating poly[(4,40-bis(2-ethylhexyl)dithieno[3,2-b:20,30-d]silole)-2,6-diyl-alt-(2,1,3-benzothiadiazole)-4,7-diyl] (PSBTBT).⁸⁶ It contained a P3HT:PC₇₁BM front sub-cell and a PSBTBT:PC₇₁BM back sub-cell. Between the sub-cells, the authors used a TiO_2 nanocrystal layer topped with an ultra-thin Al layer to improve the wettability for deposition of the back cell. An overall efficiency of 5.4% was obtained.

II.IV Use of fullerene derivatives in solar cells

Since the first use of C_{60} in polymer based photovoltaics, fullerene chemistry has been a key driver of photovoltaic efficiency. As previously mentioned, the use of $PC_{61}BM$ instead of plain C_{60} allowed the fullerene concentrations necessary to achieve a bicontinuous morphology, greatly improving device efficiency. More recently, $PC_{61}BM$ has been superseded by $PC_{71}BM$ due to its improved absorption in the visible region.^{86,87,88,89} This is because, despite the fact that the band gap of $PCC_{61}BM$ is 1.8eV, the molecule's high symmetry makes low-energy transitions formally dipole forbidden, resulting in very weak absorption of visible light.⁴⁹ The asymmetry of $PC_{71}BM$ leads to much greater absorption of visible light, with a five-fold increase in the extinction coefficient at 500nm,⁹⁰ while the HOMO and LUMO levels remain unchanged. $PC_{71}BM$ has found particular relevance in conjunction with low band-gap polymers that tend to absorb more poorly at the blue end of the visible spectrum.

Attempts to use even higher order fullerenes, such as C_{84} , which shows even greater absorption have thus far failed, due to the molecules poor solubility, even with the addition of solubilising groups.⁹⁰

Aside from the use of higher order fullerenes, researchers have investigated a wide range of C_{60} based derivatives, beyond the most commonly used [6,6]-Phenyl C_{61} butyric acid methyl ester (PCBM). The main aim of this chemistry has been to obtain a desired level of miscibility with a specific polymer donor material, thereby facilitating an 'ideal' morphology that is thermodynamically and/or kinetically favourable.⁴⁹ Approaches so far have included altering the

nature of the alkyl ester (methyl to hexadecyl),⁹¹ and the use of alkylated diphenylene moieties⁹² among others⁹³. However, to date the majority of novel C₆₀ derivatives have shown no advantage over PC₆₁BM. Two approaches that have shown some potential are the use of dihydronaphthylfullerenes⁹⁴ and thienyl based analogues of PC₆₁BM⁹⁵ although a theoretical understanding of what drives the relative success of these compounds is so far lacking.

Another avenue under investigation is to raise the fullerene LUMO, in order to optimise the open circuit voltage. As can be seen in Figure 11, in the P3HT:PCBM system, the P3HT HOMO is 5.1eV and the PCBM LUMO is 4.3eV. This sets a V_{OC} limit for this material combination of 0.8eV. Subsequently, researchers report V_{OC}s in the range of 0.58V – 0.64V^{84,96,97,98} with the shortfall ascribed to the energy required to overcome the exciton binding energy⁹⁹, and resistive losses through the device, principally at the polymer electrode interfaces.

Significant gains in V_{OC}, and therefore device efficiency, can be expected from increasing the HOMO_{donor}-LUMO_{acceptor} separation. This can be achieved by either raising the fullerene LUMO or lowering the polymer HOMO. As P3HT is the primary light-absorbing species, manipulation of the HOMO_{donor} carries the added complexity of affecting the absorption onset. In addition, the synthesis of new conjugated polymers is a difficult and unpredictable process that does not yet allow for the accurate manipulation of individual properties. Fullerene chemistry on the other hand, is far more controllable and over the last three or four years a variety of novel fullerene derivatives have been synthesised that allow for manipulation of the LUMO_{acceptor} level.

The $\text{LUMO}_{\text{donor}} - \text{LUMO}_{\text{acceptor}}$ offset must exceed the exciton binding energy, E_B , in order for charge transfer at the donor-acceptor interface to be energetically favourable⁹⁹. It has been reported that for the P3HT:PCBM system, $E_B = 0.3\text{eV}$ ⁵⁴ which leaves an extra 0.8eV over which the $\text{LUMO}_{\text{acceptor}}$ level can be raised. As such, the application of fullerene species with novel exohedral chemistry is a very promising route for improving the open circuit voltage, and therefore the efficiency, of polymer fullerene composite solar cells.

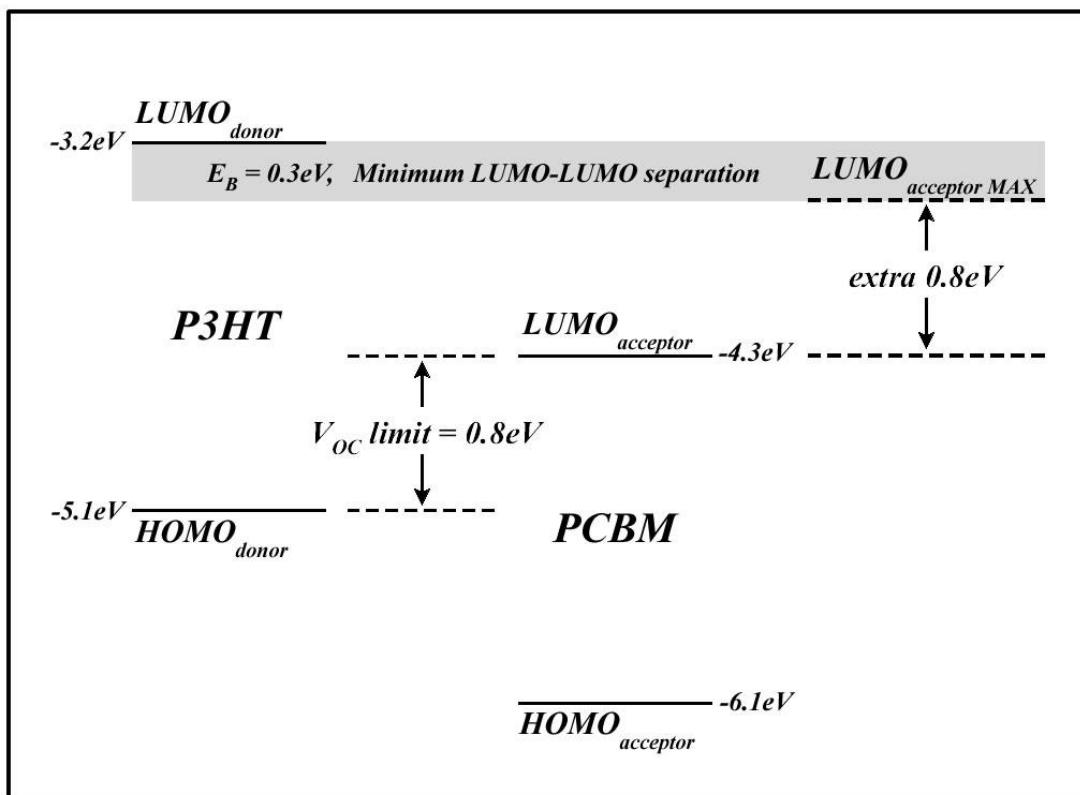


Figure 11. Energy Level Diagram of the P3HT:PCBM system showing the $\text{LUMO}_{\text{donor}} - \text{LUMO}_{\text{acceptor}}$ gap of 0.8eV which limits the V_{OC} . If only a 0.3eV LUMO-LUMO gap is required to ensure efficient exciton dissociation, an extra 0.8eV is available for the $\text{LUMO}_{\text{donor}} - \text{LUMO}_{\text{acceptor}}$ gap, if the acceptor LUMO can be raised to include it.

One approach has been to add multiple functional groups to the fullerene cage. Each addition requires the breaking of a double bond which appears to raise the molecules LUMO. Bis-adduct,¹⁰⁰ and more recently, tris-adduct¹⁰¹ fullerene derivatives have been synthesised and incorporated into photovoltaic devices with P3HT, achieving open circuit voltages of 0.73V¹⁰⁰ and 0.81V¹⁰¹ respectively. However, these gains come at a cost as space charge limited current measurements have shown that the electron mobility of the fullerene derivative decreases with the addition of each additional adduct. As such, despite the impressive open circuit voltage, devices containing tris-PC₆₁BM exhibited a very poor short circuit current and fill factor.¹⁰¹ This would suggest that exohedral modification of the fullerene cage is, as a method of increasing the fullerene LUMO, ultimately constrained by mobility concerns. It is worthwhile to note however that the work presented in reference 85 used devices spin cast from chloroform, a relatively poor solvent for polymer:fullerene solar cells. The use of a slower drying solvent such as di-chlorobenzene may allow for improved charge mobility and improved device efficiencies in higher-adduct fullerene derivatives.

A second approach to raising the fullerene LUMO is endohedral modification, whereby an atom or molecule is introduced inside the fullerene cage. To date, the most impressive results achieved with this technique have occurred through the use of trimetallic nitride compounds such as Lu₃N within a C₈₀ cage (written as Lu₃N@C₈₀).¹⁰² Neither the C₈₀ cage, nor the planar, pyramidal Lu₃N exist as separate entities, yet they form a stable molecule when combined. Cyclic voltammetry experiments have shown that the solubilised derivatives of Lu₃N@C₈₀ have

significantly higher LUMO levels than PC₆₁BM and they have been used in conjunction with P3HT to produce solar cells with open circuit voltages of 0.89V and overall efficiencies of 4.2%.¹⁰²

In this case, the draw-back is the very low synthetic yields which have limited the practical implementation of these fullerenes across a range of electronic applications. In addition, the incorporation of rare-earth elements may add significant cost to the production of these devices.

II.V Conclusion

Polymer based PV devices belong to the third generation of solar cell development and are driven by the goal of moderate efficiency at low cost. Polymer based bulk heterojunction devices first appeared in the 1990s, and today, the most impressive of these devices achieve efficiencies of nearly 7% at AM1.5 conditions.

The devices are based on semiconducting, conjugated polymers, which are distinguished by an alternating backbone of single and double bonds. The semiconducting properties arise due to the stimulated transition of electrons from localized π orbitals to the overlapping, delocalised π^* orbitals. A multitude of conjugated polymers exist for use in PVs, with the most commonly used to date being P3HT. Through the development of donor-acceptor polymers, such as the benzothiadiazole and benzodithiophenes, researchers have sought, with significant success, to optimise the polymer band gap and HOMO level in order to maximize the photocurrent and open circuit voltage respectively.

The basic photophysics of polymer based PV devices differ significantly from those of conventional semiconductor PVs. In particular, their relatively low dielectric constants and the small Bohr radii of charge carriers lead to the formation of an electrostatically bound, mobile excited state known as an exciton instead of free charge carriers upon photon absorption. As such, a polymer based PV device requires a Type II heterojunction in order to efficiently separate charge carriers. In addition, the charge concentrations generated at the heterojunction and the

relatively low charge mobilities of these polymers mean that the spatial gradient of the chemical potential, $\nabla\mu$, can be a significant driving force for charge transport.

The three primary device architectures; single layer, bilayer and bulk heterojunction have been discussed. Of these, the bulk heterojunction architecture, where the two materials that form the Type II heterojunction are intimately mixed throughout the active layer, has yielded the most promising results thus far. Lately, tandem based solar cells have also appeared in the literature, allowing significantly enhanced efficiencies, albeit at the expense of considerably more complex fabrication processes.

C₆₀, or more specifically the C₆₀ derivative PC₆₁BM, has historically been the preferred material to blend with a conjugated polymer in order to create a bulk heterojunction device. Such devices exhibit ultra-fast charge transfer and highly intermixed morphologies necessary for highly efficient bulk heterojunction solar cells. Recently, researchers have sought to move beyond PC₆₁BM. Higher order fullerenes such as PC₇₁BM and PC₈₄BM have been used to improve fullerene absorption, while endohedral and exohedral chemistry has been effectively employed to raise the fullerene LUMO and therefore the open circuit voltage, and device efficiency.

II.V References

- 1 Becquerel, A. E. *Compt. Rend. Acad. Sci.* **9**, 145 (1839).
- 2 Spanggaard, H. & Krebs, F. C. A brief history of the development of organic and polymeric photovoltaics. *Solar Energy Materials And Solar Cells* **83**, 125-146 (2004).
- 3 Martin A. Green, K. E., David L. King, Yoshihiro Hishikawa, Wilherm Warta. Solar Cell Efficiency Tables (Version 28). *Progress in Photovoltaics: Research and Applications* **14**, 445-461, doi: (2006).
- 4 Sean E. Shaheen, D. S. G., Ghassan E. Jabbour. in *MRS Bulletin* Vol. 30 10 - 15 (2005).
- 5 World Record: 41.1% efficiency reached for multi-junction solar cells at Fraunhofer ISE (Fraunhofer Institute for Solar Energy Systems ISE Freiburg 2009).
- 6 Tang., C. W. 1986. *Appl. Phys. Lett.* **48**, 183.
- 7 Oregan, B. & Gratzel, M. A Low-Cost, High-Efficiency Solar-Cell Based on Dye-Sensitized Colloidal Tio2 Films. *Nature* **353**, 737-740 (1991).
- 8 Snaith, H. J. *et al.* Efficiency Enhancements in Solid-State Hybrid Solar Cells via Reduced Charge Recombination and Increased Light Capture. *Nano Letters* **7**, 3372-3376, doi:10.1021/nl071656u (2007).
- 9 Bai, Y. *et al.* High-performance dye-sensitized solar cells based on solvent-free electrolytes produced from eutectic melts. *Nat Mater* **7**, 626-630 (2008).
- 10 Sariciftci, N. S. *et al.* Semiconducting Polymer-Buckminsterfullerene Heterojunctions - Diodes, Photodiodes, and Photovoltaic Cells. *Applied Physics Letters* **62**, 585-587 (1993).
- 11 Chyney, T. *Solarmer breaks organic solar PV cell conversion efficiency record, hits NREL-certified 7.9%*, <http://www.pvtech.org/news/_a/solarmer_breaks_organic_solar_pv_cell_conversion_efficiency_record_hits_nre/> (2009).
- 12 Sun, S. S. & Sariciftci, N. S. in *Organic Photovoltaics, Mechanisms, Materials and Devices* (Taylor and Francis Group, LLC, 2005).
- 13 Gregg, B. A. Excitonic solar cells. *Journal of Physical Chemistry B* **107**, 4688-4698 (2003).
- 14 Nelson, J. Organic Photovoltaic Films. *Current Opinion in Solid State and Materials Science* **6**, 87-95 (2002).
- 15 Hou, J., Chen, H.-Y., Zhang, S., Li, G. & Yang, Y. Synthesis, Characterization, and Photovoltaic Properties of a Low Band Gap Polymer Based on Silole-Containing Polythiophenes and 2,1,3-Benzothiadiazole. *Journal of the American Chemical Society* **130**, 16144-16145, doi:10.1021/ja806687u (2008).
- 16 Qin, R. *et al.* A Planar Copolymer for High Efficiency Polymer Solar Cells. *Journal of the American Chemical Society* **131**, 14612-14613, doi:10.1021/ja9057986 (2009).
- 17 Bijleveld, J. C. *et al.* Poly(diketopyrrolopyrrole-terthiophene) for Ambipolar Logic and Photovoltaics. *Journal of the American Chemical Society* **131**, 16616-16617, doi:10.1021/ja907506r (2009).
- 18 Park, S. H. *et al.* Bulk heterojunction solar cells with internal quantum efficiency approaching 100%. *Nat Photon* **3**, 297-302 (2009).
- 19 Hou, J. *et al.* Synthesis of a Low Band Gap Polymer and Its Application in Highly Efficient Polymer Solar Cells. *Journal of the American Chemical Society* **131**, 15586-15587, doi:10.1021/ja9064975 (2009).

- 20 Liang, Y. *et al.* Development of New Semiconducting Polymers for High Performance
Solar Cells. *Journal of the American Chemical Society* **131**, 56-57, doi:10.1021/ja808373p
(2008).
- 21 Coffin, R. C., Peet, J., Rogers, J. & Bazan, G. C. Streamlined microwave-assisted
preparation of narrow-bandgap conjugated polymers for high-performance bulk
heterojunction solar cells. *Nat Chem* **1**, 657-661 (2009).
- 22 Peet, J. *et al.* Efficiency enhancement in low-bandgap polymer solar cells by processing
with alkane dithiols. *Nat Mater* **6**, 497-500 (2007).
- 23 Markov, D. E. Ph.D. thesis, University of Groningen, The Netherlands, (2006).
- 24 Smith, R. A. *Semiconductors*. (1978).
- 25 Sun, S. S. & Sariciftci, N. S. in *Organic Photovoltaics: Mechanisms, Materials and Devices*
(Taylor and Francis Group, LLC, 2005).
- 26 Pope, M. & Swenberg, C. E. *Electronic Processes in Organic Crystals and Polymers*. 2nd
edn, (Oxford Univeristy Press, 1999).
- 27 Campbell, I. H., Hagler, T. W., Smith, D. L. & Ferraris, J. P. Direct measurement of
conjugated polymer electronic excitation energies using metal/polymer/metal structures.
Physical Review Letters **76**, 1900-1903 (1996).
- 28 Conwell, E. M. & Mizes, H. A. Photogeneration of Polaron Pairs in Conducting Polymers.
Physical Review B **51**, 6953-6958 (1995).
- 29 Sun, S. S. & Sariciftci, N. S. in *Organic Photovoltaics: Mechanisms, Materials and Devices*
(Taaylor and Francis Group, LLC, 2005).
- 30 Peumans, P., Yakimov, A. & Forrest, S. R. Small molecular weight organic thin-film
photodetectors and solar cells. *Journal of Applied Physics* **93**, 3693-3723 (2003).
- 31 Shaw, P. E., Ruseckas, A. & Samuel, I. D. W. Exciton Diffusion Measurements in Poly(3-
hexylthiophene). *Advanced Materials* **20**, 3516-3520 (2008).
- 32 Gregg, B. A. Excitonic Solar Cells. *The Journal of Physical Chemistry B* **107**, 4688-4698,
doi:10.1021/jp022507x (2003).
- 33 Mihailetchi, V. D., Koster, L. J. A., Hummelen, J. C. & Blom, P. W. M. Photocurrent
Generation in Polymer-Fullerene Bulk Heterojunctions. *Physical Review Letters* **93**,
216601 (2004).
- 34 Marsh, R. A., McNeill, C. R., Abrusci, A., Campbell, A. R. & Friend, R. H. A Unified
Description of Currentâ€“Voltage Characteristics in Organic and Hybrid Photovoltaics
under Low Light Intensity. *Nano Letters* **8**, 1393-1398, doi:10.1021/nl080200p (2008).
- 35 Dimitrakopoulos, C. D. & Mascaro, D. J. Organic thin-film transistors: A review of recent
advances. *IBM Journal of Research and Development* **45** (2001).
- 36 Sun, S. S. & Sariciftci, N. S. in *Organic Photovoltaics: Mechanisms, Materials and Devices*
(Taylor and Francis Group, LLC, 2005).
- 37 Heller, C. M., Campbell, I. H., Smith, D. L., Barashkov, N. N. & Ferraris, J. P. Chemical
potential pinning due to equilibrium electron transfer at metal/C[_{sub} 60]-doped polymer
interfaces. *Journal of Applied Physics* **81**, 3227-3231 (1997).
- 38 Zivayi, C. *Electrical and Optical Characterisation of Bulk
Heterojunction Polymer-Fullerene Solar Cells* Doctor of Natural Sciences thesis, Carl von Ossietzky
University, (2005).

- 39 Shirakawa, H., Louis, E. J., Macdiarmid, A. G., Chiang, C. K. & Heeger, A. J. Synthesis of
Electrically Conducting Organic Polymers - Halogen Derivatives of Polyacetylene, (Ch)X.
40 *Journal of the Chemical Society-Chemical Communications*, 578-580 (1977).
- Blythe, T. & Bloor, D. *Electrical Properties of Polymers*. 2 edn, (Cambridge University
41 Press, 2005).
- Rauscher, U., Bässler, H., Bradley, D. D. C. & Hennecke, M. Exciton versus band
description of the absorption and luminescence spectra in poly(p-phenylenevinylene).
42 *Physical Review B* **42**, 9830 (1990).
- Mahrt, R., Yang, J. P., Greiner, A., Bassler, H. & Bradley, D. D. C. Site-Selective
Fluorescence Spectroscopy of Poly(P-Phenylenevinylene)s and Oligomeric Model
43 Compounds. *Makromolekulare Chemie-Rapid Communications* **11**, 415-421 (1990).
- Winokur, M. J. & Chunwachirasiri, W. Nanoscale structure-property relationships in
conjugated polymers: Implications for present and future device applications. *Journal of*
44 *Polymer Science Part B-Polymer Physics* **41**, 2630-2648 (2003).
- Chen, Z. K. *et al.* A Family of Electroluminescent Silyl-Substituted Poly(p-
phenylenevinylene)s: Synthesis, Characterization, and Structure-Property Relationships.
45 *Macromolecules* **33**, 9015-9025 (2000).
- Ko, S. W., Jung, B. J., Cho, N. S. & Shim, H. K. Synthesis and characterization of new
orange-red light-emitting PPV derivatives with bulky cyclohexyl groups. *Bulletin of the*
46 *Korean Chemical Society* **23**, 1235-1240 (2002).
- Colladet, K., Nicolas, M., Goris, L., Lutsen, L. & Vanderzande, D. Low-band gap polymers
for photovoltaic applications. *Thin Solid Films* **451-52**, 7-11 (2004).
- 47 Ahn, T., Ko, S. W., Lee, J. & Shim, H. K. Novel Cyclohexylsilyl- or Phenylsilyl-Substituted
Poly(p-phenylene vinylene)s via the Halogen Precursor Route and Gilch
Polymerization. *Macromolecules* **35**, 3495-3505 (2002).
- 48 Janssen, R. A. J. in *Characterisation of Photovoltaic Materials and Devices*.
- 49 Thompson, Barry C. & Fréchet, Jean M. J. Polymer-Fullerene Composite Solar Cells.
Angewandte Chemie International Edition **47**, 58-77 (2008).
- 50 Hou, J. *et al.* Synthesis and Photovoltaic Properties of Two-Dimensional Conjugated
Polythiophenes with Bi(thienylenevinylene) Side Chains. *Journal of the American*
Chemical Society **128**, 4911-4916, doi:10.1021/ja060141m (2006).
- 51 van Müllekom, H. A. M., Vekemans, J. A. J. M., Havinga, E. E. & Meijer, E. W.
Developments in the chemistry and band gap engineering of donor-acceptor substituted
conjugated polymers. *Materials Science and Engineering: R: Reports* **32**, 1-40 (2001).
- 52 Chen, M.-H. *et al.* Efficient Polymer Solar Cells with Thin Active Layers Based on
Alternating Polyfluorene Copolymer/Fullerene Bulk Heterojunctions. *Advanced Materials*
21, 4238-4242 (2009).
- 53 Chen, H.-Y. *et al.* Polymer solar cells with enhanced open-circuit voltage and efficiency.
Nat Photon **3**, 649-653 (2009).
- 54 Scharber, M. C. *et al.* Design Rules for Donors in Bulk-Heterojunction Solar Cells -
Towards 10 % Energy-Conversion Efficiency. *Advanced Materials* **18**, 789-794 (2006).
- 55 Mandoc, M. M. *et al.* Charge transport in MDMO-PPV:PCNEPV all-polymer solar cells.
Journal of Applied Physics **101**, 104512 (2007).

- 56 Muhlbacher, D., Neugebauer, H., Cravina, A. & Sariciftci, N. S. Comparison of
Electrochemical and spectroscopic data of the low-bandgap polymer PTPTB. *Molecular*
57 *Crystals and Liquid Crystals* **385**, 85 - 92 (2002).
- 58 Weinberger, B. R. Photoconductivity, Photovoltages, and Photogenerated Solitons in
Polyacetylene. *Physical Review Letters* **50**, 1693 (1983).
- 59 Kanicki, J. & Fedorko, P. Electrical and Photovoltaic Properties of Trans-Polyacetylene.
Journal of Physics D-Applied Physics **17**, 805-817 (1984).
- 60 Glenis, S., Horowitz, G., Tourillon, G. & Garnier, F. Electrochemically grown polythiophene
and poly(3-methylthiophene) organic photovoltaic cells. *Thin Solid Films* **111**, 93-103
(1984).
- 61 Fang, Y., Chen, S.-A. & Chu, M. L. Effect of side-chain length on rectification and
photovoltaic characteristics of poly(3-alkylthiophene) Schottky barriers. *Synthetic Metals*
52, 261-272 (1992).
- 62 Marks, R. N., Halls, J. J. M., Bradley, D. D. C., Friend, R. H. & Holmes, A. B. The
photovoltaic response in poly(p-phenylene vinylene) thin-film devices. *Journal of Physics:*
Condensed Matter **6**, 1379-1394 (1994).
- 63 Yu, G., Zhang, C. & Heeger, A. J. Dual-Function Semiconducting Polymer Devices - Light-
Emitting and Photodetecting Diodes. *Applied Physics Letters* **64**, 1540-1542 (1994).
- 64 Tang, C. W. Multilayer Organic Photovoltaic Element. USA patent (1979).
- 65 Sariciftci, N. S., Smilowitz, L., Heeger, A. J. & Wudl, F. Photoinduced Electron Transfer
from a Conducting Polymer to Buckminsterfullerene. *Science* **258**, 1474-1476,
doi:10.1126/science.258.5087.1474 (1992).
- 66 Smilowitz, L. *et al.* Photoexcitation spectroscopy of conducting-polymer/C₆₀
composites: Photoinduced electron transfer. *Physical Review B* **47**, 13835 (1993).
- 67 Morita, S., Zakhidov, A. A. & Yoshino, K. Doping effect of buckminsterfullerene in
conducting polymer: Change of absorption spectrum and quenching of luminescence.
Solid State Communications **82**, 249-252 (1992).
- 68 Yoshino, K., Yin, X. H., Morita, S., Kawai, T. & Zakhidov, A. A. Enhanced photoconductivity
of C₆₀ doped poly(3-alkylthiophene). *Solid State Communications* **85**, 85-88 (1993).
- 69 Kraabel, B. *et al.* Ultrafast photoinduced electron transfer in conducting polymer--
buckminsterfullerene composites. *Chemical Physics Letters* **213**, 389-394 (1993).
- 70 Ohsawa, Y. & Saji, T. Electrochemical Detection of C₆₀(6-) at Low-Temperature. *Journal of*
the Chemical Society-Chemical Communications, 781-782 (1992).
- 71 Morita, S., Zakhidov, A. A. & Yoshino, K. Wavelength Dependence of Junction
Characteristics of Poly(3-Alkylthiophene) C-60 Layer. *Japanese Journal of Applied Physics*
Part 2-Letters **32**, L873-L874 (1993).
- 72 Halls, J. J. M., Pichler, K., Friend, R. H., Moratti, S. C. & Holmes, A. B. Exciton dissociation
at a poly(p-phenylenevinylene)/C₆₀ heterojunction. *Synthetic Metals* **77**, 277-280 (1996).
- 73 Pettersson, L. A. A., Roman, L. S. & Inganas, O. Modeling photocurrent action spectra of
photovoltaic devices based on organic thin films. *Journal of Applied Physics* **86**, 487-496
(1999).
- Lucimara S. Roman, W. M. L. A. A. P. M. R. A. O. I. High Quantum Efficiency
Polythiophene. *Advanced Materials* **10**, 774-777 (1998).

- 74 Tada, K., Onoda, M., Zakhidov, A. A. & Yoshino, K. Characteristics of poly(p-pyridyl
vinylene)/poly(3-alkylthiophene) heterojunction photocell. *Japanese Journal of Applied
Physics Part 2-Letters* **36**, L306-L309 (1997).
- 75 Kohler, A., Wittmann, H. F., Friend, R. H., Khan, M. S. & Lewis, J. Enhanced photocurrent
response in photocells made with platinum-poly-yne/C60 blends by photoinduced
electron transfer. *Synthetic Metals* **77**, 147-150 (1996).
- 76 Hummelen, J. C. *et al.* Preparation and Characterization of Fulleroid and
Methanofullerene Derivatives. *Journal of Organic Chemistry* **60**, 532-538 (1995).
- 77 Yu, G., Gao, J., Hummelen, J. C., Wudl, F. & Heeger, A. J. Polymer Photovoltaic Cells -
Enhanced Efficiencies Via a Network of Internal Donor-Acceptor Heterojunctions. *Science*
270, 1789-1791 (1995).
- 78 Shaheen, S. E. *et al.* 2.5% efficient organic plastic solar cells. *Applied Physics Letters* **78**,
841-843 (2001).
- 79 Brabec, C. J., Shaheen, S. E., Winder, C., Sariciftci, N. S. & Denk, P. Effect of LiF/metal
electrodes on the performance of plastic solar cells. *Applied Physics Letters* **80**, 1288-
1290 (2002).
- 80 Munters, T. *et al.* A comparison between state-of-the-art 'gilch' and 'sulphinyl'
synthesised MDMO-PPV/PCBM bulk hetero-junction solar cells. *Thin Solid Films* **403**, 247-
251 (2002).
- 81 Svensson, M. *et al.* High-performance polymer solar cells of an alternating polyfluorene
copolymer and a fullerene derivative. *Advanced Materials* **15**, 988-+ (2003).
- 82 Schilinsky, P., Waldauf, C. & Brabec, C. J. Recombination and loss analysis in
polythiophene based bulk heterojunction photodetectors. *Applied Physics Letters* **81**,
3885-3887 (2002).
- 83 Ma, W. L., Yang, C. Y., Gong, X., Lee, K. & Heeger, A. J. Thermally stable, efficient polymer
solar cells with nanoscale control of the interpenetrating network morphology. *Advanced
Functional Materials* **15**, 1617-1622 (2005).
- 84 Reyes-Reyes, M. *et al.* Meso-Structure Formation for Enhanced Organic Photovoltaic
Cells. *Organic Letters* **7**, 5749-5752, doi:10.1021/ol051950y (2005).
- 85 Geens, W., Aernouts, T., Poortmans, J. & Hadziioannou, G. Organic co-evaporated films of
a PPV-pentamer and C60: model systems for donor/acceptor polymer blends. *Thin Solid
Films* **403-404**, 438-443 (2002).
- 86 Sista, S. *et al.* Highly Efficient Tandem Polymer Photovoltaic Cells. *Advanced Materials* **22**,
380-383.
- 87 Kim, J. Y. *et al.* Efficient Tandem Polymer Solar Cells Fabricated by All-Solution Processing.
Science **317**, 222-225, doi:10.1126/science.1141711 (2007).
- 88 Soci, C. *et al.* Photoconductivity of a Low-Bandgap Conjugated Polymer. *Advanced
Functional Materials* **17**, 632-636 (2007).
- 89 Mühlbacher, D. *et al.* High Photovoltaic Performance of a Low-Bandgap Polymer.
Advanced Materials **18**, 2884-2889 (2006).
- 90 Kooistra, F. B. *et al.* New C84 Derivative and Its Application in a Bulk Heterojunction Solar
Cell. *Chemistry of Materials* **18**, 3068-3073, doi:10.1021/cm052783z (2006).

- 91 Zheng, L. *et al.* Methanofullerenes Used as Electron Acceptors in Polymer Photovoltaic
Devices. *The Journal of Physical Chemistry B* **108**, 11921-11926, doi:10.1021/jp048890i
(2004).
- 92 Riedel, I. *et al.* Diphenylmethanofullerenes: New and Efficient Acceptors in Bulk-
Heterojunction Solar Cells. *Advanced Functional Materials* **15**, 1979-1987 (2005).
- 93 Kooistra, F. B. *et al.* Increasing the Open Circuit Voltage of Bulk-Heterojunction Solar Cells
by Raising the LUMO Level of the Acceptor. *Organic Letters* **9**, 551-554,
doi:10.1021/ol062666p (2007).
- 94 Backer, S. A., Sivula, K., Kavulak, D. F. & Frechet, J. M. J. High Efficiency Organic
Photovoltaics Incorporating a New Family of Soluble Fullerene Derivatives. *Chemistry of*
Materials **19**, 2927-2929, doi:10.1021/cm070893v (2007).
- 95 Popescu, L. M., Hof, P. v. t., Sieval, A. B., Jonkman, H. T. & Hummelen, J. C. Thienyl analog
of 1-(3-methoxycarbonyl)propyl-1-phenyl-[6,6]-methanofullerene for bulk heterojunction
photovoltaic devices in combination with polythiophenes. *Applied Physics Letters* **89**,
213507 (2006).
- 96 Ma, W., Yang, C., Gong, X., Lee, K. & Heeger, A. J. Thermally Stable, Efficient Polymer
Solar Cells with Nanoscale Control of the Interpenetrating Network Morphology.
Advanced Functional Materials **15**, 1617-1622 (2005).
- 97 Liang, C.-W., Su, W.-F. & Wang, L. Enhancing the photocurrent in poly(3-
hexylthiophene)/[6,6]-phenyl C[₆₀] butyric acid methyl ester bulk heterojunction
solar cells by using poly(3-hexylthiophene) as a buffer layer. *Applied Physics Letters* **95**,
133303 (2009).
- 98 Li, G. *et al.* Solvent Annealing Effect in Polymer Solar Cells Based on Poly(3-
hexylthiophene) and Methanofullerenes. *Advanced Functional Materials* **17**, 1636-1644
(2007).
- 99 Rand, B. P., Burk, D. P. & Forrest, S. R. Offset energies at organic semiconductor
heterojunctions and their influence on the open-circuit voltage of thin-film solar cells.
Physical Review B (Condensed Matter and Materials Physics) **75**, 115327 (2007).
- 100 Lenes, M. *et al.* Fullerene Bisadducts for Enhanced Open-Circuit Voltages and Efficiencies
in Polymer Solar Cells. *Advanced Materials* **20**, 2116-2119 (2008).
- 101 Lenes, M. *et al.* Electron Trapping in Higher Adduct Fullerene-Based Solar Cells. *Advanced*
Functional Materials **19**, 3002-3007 (2009).
- 102 Ross, R. B. *et al.* Endohedral fullerenes for organic photovoltaic devices. *Nat Mater* **8**,
208-212 (2009).